

# Fast In-Memory SQL Analytics on Graphs

Chunbin Lin, Benjamin Mandel, Yannis Papakonstantinou, Matthias Springer  
CSE, UC San Diego

{chunbinlin, bmandel, yannis, mspringer}@cs.ucsd.edu

arXiv:1602.00033v3 [cs.DB] 11 Apr 2016

## ABSTRACT

We study a class of graph analytics SQL queries, which we call *relationship queries*. Relationship queries are a wide superset of fixed-length graph reachability queries and of tree pattern queries. A relationship query performs selections, joins and semijoins (WHERE clause subqueries) over tables that correspond to entities (i.e., vertices) and binary relationships (i.e., edges). Intuitively, it discovers target entities that are reachable from source entities specified by the query. It usually also finds aggregated scores, which correspond to the target entities and are calculated by applying aggregation functions on measure attributes, which are found on (1) the target entities, (2) the source entities and (3) the paths from the sources to the targets. We present real-world OLAP scenarios, where efficient relationship queries are needed. However, row stores, column stores and graph databases are unacceptably slow in such OLAP scenarios. We briefly comment on the straightforward extension of relationship queries that allows accessing arbitrary schemas.

The *GQ-Fast* in-memory analytics engine utilizes a bottom-up fully pipelined query execution model running on a novel data organization that combines salient features of column-based organization, indexing and compression. Furthermore, GQ-Fast compiles its query plans into executable C++ source code. Besides achieving runtime efficiency, GQ-Fast also reduces main memory requirements because, unlike column databases, GQ-Fast selectively allows more dense forms of compression including heavy-weighted compressions, which do not support random access.

We used GQ-Fast to accelerate queries for two OLAP dashboards in the biomedical field. The first dashboard runs queries on the PubMed dataset and the second one on the SemMedDB dataset. It outperforms Postgres by 2-4 orders of magnitude and outperforms MonetDB and Neo4j by 1-3 orders of magnitude when all of them are running on RAM. Our experiments dissect the GQ-Fast's advantage between (i) the use of compiled code, (ii) the bottom-up pipelining execution strategy and (iii) various data structure choices. Other analysis and experiments show the space savings of GQ-Fast due to the appropriate use of compression methods, while we also show that the runtime penalty incurred by the dense compression methods decreases as the number of CPU cores raises.

## 1. INTRODUCTION

A common type of Online Analytical Processing (OLAP) queries on graphs [15, 14, 60, 54] proceeds in three steps: First, the query selects a set of source entities that satisfy certain user-provided properties. Then, the query discovers target entities that are reachable from the source entities. If it is an SQL query (as is the case in this paper), it “navigates” between entities via join operations. During the navigation the query collects measure attributes about the nodes and the edges. In the last step, these measures are aggregated and assigned to the target entities. The resulting aggregate measures typically indicate metrics of “relevance” or “importance” of the discovered entities in the context created by the source entities. We call such queries *relationship queries*.

In the interest of further specifying the subset of SQL queries that corresponds to relationship queries, we classify the tables of an SQL schema into two categories, which correspond to the entities and the relationships of the E/R model [49, 21, 20]: *relationship tables* and *entity tables*. Each tuple of an entity table corresponds to a real-life entity, which can be thought of as a vertex in a graph. Each entity table has an ID (primary key) attribute. Relationship tables, on the other hand, capture many-to-many relationships. This paper focuses on binary relationships. Therefore a (binary) relationship table has two *foreign key attributes* referencing the IDs of respective entity tables. A relationship table may also have *measure attributes*. Each tuple of a relationship table can be thought of as one edge between the two entities referenced by the foreign key attributes. The measure attributes can be thought of as attributes of the edge. Figure 1 is a relational representation of entities and relationships in Pubmed, the premier public biomedical database<sup>1</sup>. For example, the **Term** entity table has one tuple for each term of the PubMed MeSH (Medical Subject Heading)<sup>2</sup> ontology. The relationship table **DT** has two foreign key attributes **Doc** and **Term** referring to the **ID** column of entity tables **Doc** and **Term**. The measure attribute **Fre** stands for “frequency”. A tuple  $(d, t, f)$  indicates that the term  $t$  appears in the document  $d$ ,  $f > 0$  times.

An SQL query over relationship tables and entity tables, is a relationship query if (1) in its algebraic form, it involves  $\sigma$ ,  $\pi$ ,  $\bowtie$ ,  $\times$  operators and an optional aggregation operator  $\gamma$  at the end; (2) each join and semijoin condition involves an equality between (primary or foreign) key attributes and (3) aggregations group-by on a single primary key or foreign key. Notice, the set of relationship queries includes bounded-length graph reachability (path finding) queries and tree pattern queries, where the graph is SQL-encoded, i.e., the edges are defined by foreign keys. The restrictions (1-3) are commonly met in practice. In particular, most joins are based on primary keys and foreign keys) and do not prevent relationship

<sup>1</sup><http://www.ncbi.nlm.nih.gov/pubmed>

<sup>2</sup><https://www.nlm.nih.gov/bsd/disted/meshtutorial/themeshdatabase/>

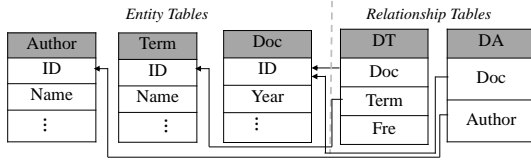


Figure 1: **Entities and relationships in Pubmed.**

queries from having wide applications. Furthermore, we show that restriction (3) can be removed at a minor cost. Section 4 formally defines the wide class of relationship SQL queries and argues for its prevalence. It provides a variety of real-life applications and queries relating to PubMed [29] and the SemMedDB [30] biomedical knowledge databases.

Next we illustrate a relationship query. Given the very high volume of publications (more than 23M) and authors (more than 6.3M) in PubMed, one may want to issue the following *Author Similarity (AS)* relationship query that finds authors that publish on the same topics with the author with ID 7. More precisely, the query finds the authors (identified by **da2.Author**) whose publications (identified by **d.ID**) relate to the MeSH terms (identified by **dt1.Term**) in the publications **da1.Doc** of the author 7. Furthermore, each discovered author is given a weight/similarity score, by first computing the similarity of her publications’ terms to the terms of the publications of author 7. The similarity function is a typical cosine-based: Conceptually there is a vector  $v^i = [t_1^i, \dots, t_m^i]$  for each author  $a_i$ ;  $t_j^i$  is the number of times that the term  $t_j$  appeared in the publications of  $a_i$ . Then the similarity between authors  $a_1$  and  $a_2$  is the cosine of the vectors  $v^1$  and  $v^2$ . Additional weight is given to recent publications.<sup>3</sup>

AS query:

```
SELECT da2.Author, SUM(dt1.Fre×dt2.Fre) / (2017-d.Year)
FROM ( ( DA da1 JOIN DT dt1 ON da1.Doc=dt1.Doc)
      JOIN DT dt2 ON dt1.Term = dt2.Term)
      JOIN Doc d ON dt2.Doc=d.ID)
      JOIN DA da2 ON dt2.Doc=da2.Doc
WHERE da1.Author = 7
GROUP BY da2.Author
```

Given the analytical nature of relationship queries, column-oriented database systems are much more efficient than row-stores and graph databases, as our experiments verified (see Section 7) [50, 7, 5, 6, 27, 42]. Nevertheless, the obtained performance is often not sufficient for online queries and interactive applications. For example, the AS query takes 1.24 hours on the column database MonetDB [27], 8.20 hours on the row database Postgres<sup>4</sup> [38], and 2.05 hours on the graph database Neo4j<sup>5</sup>, [55], even though we fully cached the data in main memory in all of them. In contrast, GQ-Fast executes the AS query in just 5.66 seconds, which presents an improvement of many orders of magnitude. Furthermore, we show that the space requirements of GQ-Fast are generally lower. Section 4 provides multiple additional examples of OLAP relationship queries.

GQ-Fast achieves such superior performance by combining a novel fragment-based data structure with a novel type of compiled

<sup>3</sup>For simplicity, we ignore that in practice the weight function adjusts frequency to whether the actual content of the paper is available or just the abstract. In practice, we also use a log-based adjustment of frequency.

<sup>4</sup><http://www.postgresql.org/>

<sup>5</sup><http://neo4j.com/>

execution plans. Generally, for each binary relationship table  $R(F_1, F_2, M_1, \dots, M_m)$  where  $F_1, F_2$  are foreign keys and each  $M_i$  is a measure, GQ-Fast conceptually (but not physically) makes two copies  $R_1$  sorted by  $F_1$  and  $R_2$  sorted by  $F_2$ . Physically, GQ-Fast makes an index  $\mathcal{I}_{R.F_1}$  corresponding to  $R_1$  and an  $\mathcal{I}_{R.F_2}$  corresponding to  $R_2$ . Assuming  $F_1$  has  $n$  unique values  $t_1, \dots, t_n$ , GQ-Fast produces  $n$  fragments  $\pi_{F_2 \sigma_{F_1=t_i}}(R_1)$  and  $n \times m$  fragments  $\pi_{M_j \sigma_{F_1=t_i}}(R_1)$ . A fragment is a list of values potentially with duplicates. Figure 2 shows example indices and fragments for the schema in Figure 1. The index  $\mathcal{I}_{DA.Author}$  associates the **Author** entity 7 with the **DA.Doc** fragment  $\pi_{Doc \sigma_{Author=7}}(DA)$ . Note that, this new organization allows GQ-Fast to directly obtain values (eg, document IDs) that are associated to a given value (eg, the given author ID 7), without accessing row ids.

For space saving reasons explained later, the fragments of an attribute are stored consecutively but encoded separately in large byte arrays. For example, the **DA.Doc** byte array (of the  $\mathcal{I}_{DA.Author}$  index) contains the values of the **DA.Doc** attribute. Therefore, at a first glance, it appears as if the **DA.Doc** is identical to a column in a column database. However, there is an important difference, which is motivated by this key observation: GQ-Fast query plans do not need random access within any individual fragment of the **DA.Doc** byte array. Rather, when a fragment (say,  $\pi_{Doc \sigma_{Author=7}}(DA)$ ) is accessed, all its data will be used. Based on this observation, GQ-Fast allows dense encodings of each individual fragment, such as Huffman encoding [26, 51, 17]. Such encodings do not allow random access within the fragment. Note that a typical fragment has relatively small size and can typically fit in the L1 cache or, at least, in the L2 cache. Hence, its decoding is not penalized with random accesses to the RAM.

Still, plans for relationship queries need efficient access to whole fragments, i.e., need to efficiently find their start and end. This is achieved by the offset-based lookup tables of the GQ-Fast indices. Section 5 further discusses aspects of the GQ-Fast indices, which lead to runtime performance and space savings.

The GQ-Fast query plans run on the indices (exclusively). They essentially employ a bottom-up pipelined execution model to avoid large intermediate results. In addition, GQ-Fast employs a code generator to compile the query plan into executable C++ code. The compiled code utilizes simple for-loops to access the elements in a fragment. Such tight for-loops without function calls create high instruction locality which eliminates the instruction cache-miss problem. In addition, such simple loops are amenable to compiler optimization, and CPU out-of-order speculation [5, 27].

As an example, consider the code of Figure 3 that is the result of code generation for the AS query. The Figure uses variable names that indicate their relationship to the tuple variables (**da1**, **dt1**, **dt2**, **d** and **da2**) of the query. Notice that the AS query has only joins and aggregation. Other cases, involving semijoins and intersection are discussed later.

First, in (Lines 2 to 9) GQ-Fast uses the  $\mathcal{I}_{DA.Author}$  index to find that the document-fragment  $\pi_{Doc \sigma_{Author=7}}(DA \mapsto da1)$  starts at the position offset  $\mathcal{F}_{da1.Doc}$  (see Figure 2) which is the offset in the 7-th position of the **DA.Author** lookup table. The encoded fragment length  $l_{da1.Doc}$  is computed by subtracting the offset of the 7-th position from the offset of the 8-th position. GQ-Fast proceeds to decode the fragment into the (preallocated) array  $\mathcal{A}_{da1.Doc}$ .

Then, in the inner loop of Lines 10 to 19, for each document ID  $v_{da1.Doc} \in \mathcal{A}_{da1.Doc}$ , GQ-Fast uses the index  $\mathcal{I}_{DT.Doc}$  to find the term-fragment  $\pi_{dt1.Term \sigma_{dt1.Doc=v_{da1.Doc}}}(DT \mapsto dt1)$ , which starts from the position offset  $\mathcal{F}_{dt1.Term}$  of the **DT.Term** byte array (see example of Figure 2); similarly, it also finds the frequency-fragment  $\pi_{dt1.Fre \sigma_{dt1.Doc=v_{da1.Doc}}}(DT \mapsto dt1)$ . For example, since

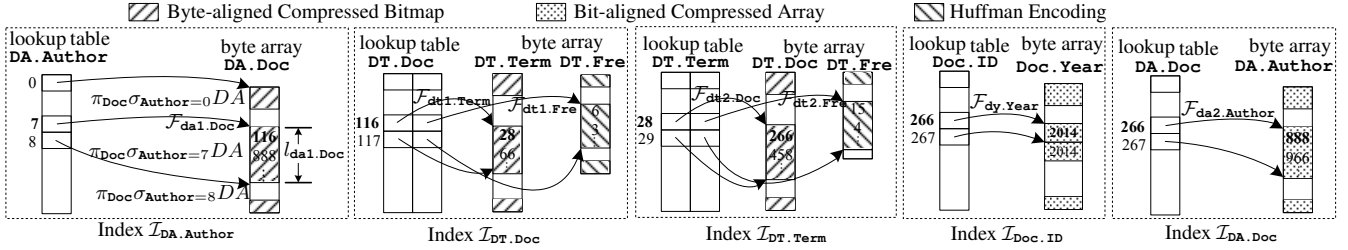


Figure 2: **Example of fragments and query processing.** Fragment  $\pi_{\text{Doc}}\sigma_{\text{Author}=7}\text{DA}$  is encoded with byte-aligned bitmap while fragments  $\pi_{\text{Term}}\sigma_{\text{Doc}=116}\text{DT}$  and  $\pi_{\text{Fre}}\sigma_{\text{Doc}=116}\text{DT}$  are encoded by Bit-aligned compressed array and Huffman encoding respectively.

the document id 116 appears in the decoded  $\pi_{\text{Doc}}\sigma_{\text{Author}=7}\text{DA}$ , GQ-Fast finds the corresponding offsets  $\mathcal{F}_{\text{dt1.Term}}$  and  $\mathcal{F}_{\text{dt1.Fre}}$  in the 116-th position of the  $\text{DT.Doc}$  lookup table. Then GQ-Fast decodes the identified fragments into  $\mathcal{A}_{\text{dt1.Term}}$  and  $\mathcal{A}_{\text{dt1.Fre}}$ .

Intuitively, at this point, the two outer loops have identified the documents, terms and frequencies associated with the tuple variables  $\text{da1}$  and  $\text{dt1}$  of the query. Similarly, the inner loops identify the attributes associated with the tuple variables  $\text{dt2}$ ,  $\text{d}$  and  $\text{da2}$ . The innermost loop utilizes the current values of the attributes that appear in the **SELECT** clause in order to update the sum aggregates in the array  $\text{mathcal{R}}$ . Notice that since the group-by list is a single key, it is sufficient to use an array for the final aggregation. The size of such array is the domain size of **Author.ID**. Assuming consecutive author IDs, this simply the number of authors.

In particular, for each term  $v_{\text{dt1.Term}} \in \mathcal{A}_{\text{dt1.Term}}$ , GQ-Fast decodes a fragment  $\pi_{\text{dt2.Doc}}\sigma_{\text{dt2.Term}=v_{\text{dt1.Term}}}(\text{DT} \mapsto \text{dt2})$  in the  $\text{DT.Doc}$  byte array starting from position offset  $\mathcal{F}_{\text{dt2.Doc}}$  and a fragment  $\pi_{\text{dt2.Fre}}\sigma_{\text{dt2.Term}=v_{\text{dt1.Term}}}(\text{DT} \mapsto \text{dt2})$  in the  $\text{DT.Fre}$  byte array starting from position offset  $\mathcal{F}_{\text{dt2.Fre}}$  on index  $\mathcal{I}_{\text{DT.Term}}$ . For example, for term id 28, GQ-Fast gets the offsets  $\mathcal{F}_{\text{dt2.Doc}}$  and  $\mathcal{F}_{\text{dt2.Fre}}$  in the 28-th position in the  $\text{DT.Term}$  lookup table.

For each document  $v_{\text{dt2.Doc}} \in \mathcal{A}_{\text{dt2.Doc}}$ , GQ-Fast decodes a fragment  $\pi_{\text{dy.Year}}\sigma_{\text{dy.ID}=v_{\text{dt2.Doc}}}(\text{Doc} \mapsto \text{dy})$  in the  $\text{Doc.Year}$  byte array, which starts from position offset  $\mathcal{F}_{\text{dy.Year}}$  on index  $\mathcal{I}_{\text{Doc.ID}}$ , and also decodes a fragment  $\pi_{\text{da2.Author}}\sigma_{\text{da2.Doc}=v_{\text{dt2.Doc}}}(\text{DA} \mapsto \text{da2})$  in the  $\text{DA.Author}$  byte array, which starts from position offset  $\mathcal{F}_{\text{DA.Doc}}$  on index  $\mathcal{I}_{\text{DA.Doc}}$ . For example, for document id 266, GQ-Fast gets the offsets  $\mathcal{F}_{\text{dy.Year}}$  and  $\mathcal{F}_{\text{da2.Author}}$  in the 266-th position in the  $\text{Doc.ID}$  and  $\text{DA.Doc}$  lookup tables respectively.

Finally, for each author  $v_{\text{da2.Author}}$ , GQ-Fast calculates the aggregated score  $\sum(v_{\text{da1.Fre}} \times v_{\text{da2.Fre}})/(2017 - v_{\text{dy.Year}})$  and inserts it into the result set  $\mathcal{R}$ .

**Contributions.** GQ-Fast introduces multiple coordinated novelties that lead to runtime performance, space savings, or both, in the case of graph analytics.

- Section 4 formally *defines relationship queries*, a class of OLAP graph queries that are prevalent in practice, as illustrated in two real-world use cases.
- Section 5 introduces a new *fragment-based data organization*, which combines features of the column data organization and indexing. This data organization gets rid of row ids. Based on the observation that plans need to efficiently find a fragment but do not need random access within the fragment, GQ-Fast allows for aggressive compressions of fragments, such as compressed bitmaps and Huffman encoding. Therefore, more data can fit in the main memory. We study the space cost of the used compression algorithms and show that it is relatively easy to choose between them.

- Section 6 shows how GQ-Fast query plans are *compiled into code* (C++). Furthermore, this code uses *bottom-up pipelining* to evaluate the query, effectively avoiding the materialization of intermediate results. More precisely, whereas a column database (see discussion in Section 2) would create intermediate results for row IDs and/or columns of intermediate results, in GQ-Fast’s bottom-up pipelining, each intermediate result is a scalar variable of the compiled C++ code, hence being efficiently stored and accessed via a CPU register. The combination of compiled code and bottom-up pipelining further amplifies benefits of compiled code, such as high instruction locality and out-of-order speculation.
- The data organization (Section 5), as well as the plans, are further *optimized by tuning to the dense IDs*, i.e., tuning to the fact that the entities’ IDs are consecutive integers.
- We present a comprehensive set of experiments on three real-life datasets, i.e., PubMed-M, PubMed-MS and SemmedDB. The results show that GQ-Fast is  $10^2 \sim 10^4$  more efficient than MonetDB, Neo4j and Postgres when they all run on main memory.
- As is obvious from the above contributions list, the runtime performance advantage of GQ-Fast is affected by multiple factors: bottom-up pipelining, compiled code, dense IDs, aggressive compression.<sup>6</sup> Therefore, a next series of experiments isolates the effect of individual factors producing multiple important observations: First, the vast majority of the runtime performance advantage is due to the combination of compilation with bottom-up pipelining, while the dense IDs optimization has a secondary role. Second, the use of aggressive compressions will become more useful as the number of cores in CPUs increases rapidly (hence reducing the decoding penalty), while the RAM-to-CPU bandwidth improves significantly slower.
- We deployed GQ-Fast in two real world use cases, around the PubMed and SemMedDB data. An online and interactive demo system is also provided <http://137.110.160.52:8080/demo> for the reader to experience the benefit of GQ-Fast in online graph analytics.

**Roadmap** Section 2 describes related work. It emphasizes the necessary background on compression. It also illustrates the limitations of column databases by providing a detailed step-by-step description of how an exemplary column database would answer the AS query. Section 4 introduces the schema and relationship queries, respectively. Section 3 illustrates the architecture of GQ-Fast. We describe the structure of the GQ-Fast index and theoretically analyzes different compressions in Section 5. Section 6 describes the GQ-Fast code generator. Finally, Section 7 conducts

<sup>6</sup>This is alike column databases, where multiple contributions converged to their performance benefits.

Example algorithm for AS query

```

1  $\mathcal{R} \leftarrow \emptyset$ ;  $\mathcal{R}$  is an array and is initialized to all zeros
    $|\mathcal{R}|$  is the domain size of da2.Author
2 offset-array  $\mathcal{P}_{da1} = \mathcal{I}_{DA.Author} [7]$ ;  $\mathcal{P}_{da1}$  is a user-provided input
3 BB-encoded fragment  $\mathcal{F}_{da1.Doc} = \mathcal{P}_{da1}[\mathbf{column}(\mathbf{Doc})]$ ;
4 offset-array  $next = \mathcal{I}_{DA.Author} [7+1]$ ;
5 length  $l_{da1.Doc} = next[\mathbf{column}(\mathbf{Doc})] - \mathcal{F}_{da1.Doc}$ ;
6 decodeBB( $\mathcal{F}_{da1.Doc}, l_{da1.Doc} : A_{da1.Doc}, n_{da1.Doc}$ );
7  $\mathit{lldecodeBB}()$  is a macro
8  $\mathit{llA}_{da1.Doc}$  is now the array with the decoded fragment
9  $\mathit{llm}_{da1.Doc}$  is the number of elements in  $A_{da1.Doc}$ 
10 for  $i_{da1.Doc} = 0; i_{da1.Doc} < n_{da1.Doc}; i_{da1.Doc} ++$  do
11    $v_{da1.Doc} = A_{da1.Doc}[i_{da1.Doc}]$ ;
12   offset-array  $\mathcal{P}_{dt1} = \mathcal{I}_{DT.Doc}[v_{da1.Doc}]$ ;
13   BB-encoded fragment  $\mathcal{F}_{dt1.Term} = \mathcal{P}_{dt1}[\mathbf{column}(\mathbf{Term})]$ ;
14   offset-array  $next = \mathcal{I}_{DT.Doc}[v_{da1.Doc} + 1]$ ;
15   length  $l_{dt1.Term} = next[\mathbf{column}(\mathbf{Term})] - \mathcal{F}_{dt1.Term}$ ;
16   decodeBB( $\mathcal{F}_{dt1.Term}, l_{dt1.Term} : A_{dt1.Term}, n_{dt1.Term}$ );
17   Huffman-encoded fragment  $\mathcal{F}_{dt1.Fre} = \mathcal{P}_{dt1}[\mathbf{column}(\mathbf{Fre})]$ ;
18   length  $l_{dt1.Fre} = next[\mathbf{column}(\mathbf{Fre})] - \mathcal{F}_{dt1.Fre}$ ;
19   decodeHuffman( $\mathcal{F}_{dt1.Fre}, l_{dt1.Fre} : A_{dt1.Fre}, n_{dt1.Fre}$ );
20   for  $i_{dt1.Term} = 0; i_{dt1.Term} < n_{dt1.Term}; i_{dt1.Term} ++$  do
21      $v_{dt1.Term} = A_{dt1.Term}[i_{dt1.Term}]$ ;
22      $v_{dt1.Fre} = A_{dt1.Fre}[i_{dt1.Term}]$ ;
23     offset-array  $\mathcal{P}_{dt2} = \mathcal{I}_{DT.Term}[v_{dt1.Term}]$ ;
24     BB-encoded fragment  $\mathcal{F}_{dt2.Doc} = \mathcal{P}_{dt2}[\mathbf{column}(\mathbf{Doc})]$ ;
25     offset-array  $next = \mathcal{I}_{DT.Term}[v_{dt1.Term} + 1]$ ;
26     length  $l_{dt2.Doc} = next[\mathbf{column}(\mathbf{Doc})] - \mathcal{F}_{dt2.Doc}$ ;
27     decodeBB( $\mathcal{F}_{dt2.Doc}, l_{dt2.Doc} : A_{dt2.Doc}, n_{dt2.Doc}$ );
28     Huffman-encoded fragment  $\mathcal{F}_{dt2.Fre} = \mathcal{P}_{dt2}[\mathbf{column}(\mathbf{Fre})]$ ;
29     length  $l_{dt2.Fre} = next[\mathbf{column}(\mathbf{Fre})] - \mathcal{F}_{dt2.Fre}$ ;
30     decodeHuffman( $\mathcal{F}_{dt2.Fre}, l_{dt2.Fre} : A_{dt2.Fre}, n_{dt2.Fre}$ );
31     for  $i_{dt2.Doc} = 0; i_{dt2.Doc} < n_{dt2.Doc}; i_{dt2.Doc} ++$  do
32        $v_{dt2.Doc} = A_{dt2.Doc}[i_{dt2.Doc}]$ ;
33        $v_{dt2.Fre} = A_{dt2.Fre}[i_{dt2.Doc}]$ ;
34       offset-array  $\mathcal{P}_{dy} = \mathcal{I}_{Doc.ID}[v_{dt2.Doc}]$ ;
35       BCA-encoded fragment  $\mathcal{F}_{dy.ID} = \mathcal{P}_{dy}[\mathbf{column}(\mathbf{ID})]$ ;
36       offset-array  $next = \mathcal{I}_{Doc.ID}[v_{dt2.Doc} + 1]$ ;
37       length  $l_{dy.ID} = next[\mathbf{column}(\mathbf{Year})] - \mathcal{F}_{dy.ID}$ ;
38       decodeBCA( $\mathcal{F}_{dy.ID}, l_{dy.ID} : A_{dy.ID}, n_{dy.ID}$ );
39        $v_{dy.Year} = A_{dy.Year}[0]$ ;
40       offset-array  $\mathcal{P}_{da2} = \mathcal{I}_{DA.Doc}[v_{dt2.Doc}]$ ;
41       BD-encoded fragment  $\mathcal{F}_{da2.Author} = \mathcal{P}_{da2}[\mathbf{column}(\mathbf{Author})]$ ;
42       offset-array  $next = \mathcal{I}_{DA.Author}[v_{da2.Author} + 1]$ ;
43       length  $l_{da2.Author} = next[\mathbf{column}(\mathbf{Author})] - \mathcal{F}_{da2.Author}$ ;
44       decodeBCA( $\mathcal{F}_{da2.Author}, l_{da2.Author} : A_{da2.Author}, n_{da2.Author}$ );
45       for  $i_{da2.Author} = 0; i_{da2.Author} < n_{da2.Author}; i_{da2.Author} ++$  do
46          $v_{da2.Author} = A_{da2.Author}[i_{da2.Author}]$ ;
47          $\mathcal{R}[v_{da2.Author}] += \frac{(v_{dt1.Fre} * v_{dt2.Fre})}{2017 - v_{dy.Year}}$ ;
48 Return  $\mathcal{R}$ ;

```

Figure 3: Example GQ-Fast code for the AS query

comprehensive experiments to measure the performance in three real-life datasets.

## 2. RELATED WORK

We illustrate the operation of an exemplary column database during execution of the AS query, highlighting relevant optimizations [3, 6] and limitations. (Readers familiar with column databases can skip this part). We employ the modern column database storage strategy—using virtual IDs instead of explicit row ids (Explicit row ids blot the size of data) for each separately storing column. To access the  $i$ -th value in column  $C$  simply requires a random access at the location  $startOf(C) + i \times width(C)$ . Note that, columns here have fixed width, since columns are dictionary-encoded first if they are not integers.

In a convention followed across the full paper, the leaves of algebraic expressions have the form “ $table \mapsto variable$ ”. Consequently, the other operators use the “ $variable.attribute$ ” notation. For readability, the variables have the same names with the tuple variables of the **FROM** clause of the respective queries.

First, we describe the case where there is no sorting and no indices for the **DA** and **DT** tables.

1. Obtain  $\mathcal{R}_1 = \pi_{Doc} \sigma_{Author=7}(\mathbf{DA} \mapsto \mathbf{da1})$ : First scan the column **DA.Author** to find the set of row IDs  $RID_1$  associated with the author 7. Then performing random accesses on column **DA.Doc** to get the document ID’s for every row in  $RID_1$ . Note that  $\mathcal{R}_1$  is materialized.
2. Obtain  $\mathcal{R}_2 = \pi_{dt1.Term, dt1.Fre}(\mathcal{R}_1 \bowtie (DT \mapsto dt1))$ . For each document ID  $d \in \mathcal{R}_1$ , scan the column **DT.Doc** to find the set of row IDs  $RID_2$  referring to  $d$ . Retrieve the term ID and term frequency for every row in  $RID_2$  using random access on **DT.Term** and **DT.Fre**, respectively.  $RID_2$  and  $\mathcal{R}_2$  are materialized.
3. Obtain  $\mathcal{R}_3 = \pi_{dt2.Doc, \mathcal{R}_2.Fre \rightarrow Fre1, dt2.Fre \rightarrow Fre2}(\mathcal{R}_2 \bowtie (DT \mapsto dt2))$ . For each term ID  $t \in \mathcal{R}_2.Term$ , scan column **DT.Term** to find the set of row IDs  $RID_3$  referring to  $t$ . Retrieve the term ID and term frequency for every row in  $RID_3$  using random accesses on **DT.Doc** and **DT.Fre**, respectively.  $RID_3$  and  $\mathcal{R}_3$  are materialized.
4. Obtain  $\mathcal{R}_4 = \pi_{\mathcal{R}_3.Doc, \mathcal{R}_3.Fre1, \mathcal{R}_3.Fre2, d.Year}(\mathcal{R}_3 \bowtie (Document \mapsto d))$ . For each document ID  $d \in \mathcal{R}_3.Doc$ , scan column **Document.ID** to find the set of row IDs  $RID_4$  referring to  $d$ . Retrieve the publishing year for every row in  $RID_4$  using random access on **Document.ID**.  $RID_4$  and  $\mathcal{R}_4$  are materialized.
5. Obtain  $\mathcal{R}_5 = \pi_{da2.Author, \mathcal{R}_4.Fre1, \mathcal{R}_4.Fre2, \mathcal{R}_4.Year}(\mathcal{R}_4 \bowtie DA \mapsto da2)$ . For each document ID  $d \in \mathcal{R}_4.Doc$ , scan column **DA.doc** to find the set of row IDs  $RID_5$  referring to  $d$ . Retrieve the author ID for every row in  $RID_5$  using random access on **DT.Author**.  $RID_5$  and  $\mathcal{R}_5$  are materialized.
6. Calculate  $\mathcal{R}_6 = \gamma_{Author, SUM(Fre1.Fre2)} / (2017 - Year)(\mathcal{R}_5)$ . Scan  $\mathcal{R}_5$  to get the set of distinct authors and associated scores  $\sum(Fre1.Fre2) / (2017 - Year)$ .

The above example exhibits a number of inefficiencies.

1. Expensive scanning operations are executed. Step 1~5 obtain explicit or implicit row ids via whole column scanning.
2. Intermediate results are maintained. Steps 1~5 materialize all the temporary output results  $\mathcal{R}_1, \dots, \mathcal{R}_5$  and also row ids  $RID_2, \dots, RID_5$ , which is both time and space consuming.

To speedup the performance of the above example, many existing optimizations can be applied, e.g., late tuple materialization, block iteration, invisible joins and column-specific compression schemes [4, 7, 5, 6, 27, 3]. In this paper, these optimizations are all utilized in our baselines. Note that, we do not build hash index in our baselines, since we mainly work on relationship tables, each individual column in a relationship table is not a primary key and has many duplicates.

For instance, to eliminate whole column scan, binary search can be utilized [12, 32] if the column is sorted. Since we adopt the virtual IDs store strategy, all the columns should be organized in one order. That is binary search only works for one column. However, relationship queries might perform lookup operation in two reference columns. To avoid whole column scan in both columns, two copies of data with different sorting should be maintained (as we did for GQ-Fast and OMC, more details can be found in 7).

**Data Compression Schemes** Column databases do not consider heavy-weight data compression schemes, since they do not allow partial decompression - hence requiring that the whole column (or block) should be decompressed whenever data of the column are needed. The archetypical heavy-weight compression scheme is

Huffman encoding [26, 51, 17]. In the context of our comparisons, OMC does not use heavy-weight compression schemes, while GQ-Fast does, when beneficial. We list below the compression schemes used in column databases and in GQ-Fast .

**Dictionary encoding.** The most widely utilized dictionary encoding maintains a global mapping table to map each wide value to an integer. For example, a simple dictionary for a string-typed column of states might map “Alabama” to 0, “Alaska” to 1, “Arizona” to 2, and so on [28, 47, 62, 4]. GQ-Fast applies a dictionary encoding to map string-type columns to integers upon load time, so GQ-Fast only processes integer columns in query processing phase. GQ-Fast also applies a variant of bit-aligned dictionary encoding on fragments, which will be discussed in Section 5.

**Run-length encoding.** The traditional run-length encoding (RLE) expresses the repeats of the same element as (value, run-length) [51, 3, 4]. Assume a column  $R.A$  of  $R(A,B)$  is compressed by this standard RLE, then the whole column should be decompressed to answer the projection-selection query  $\pi_B \sigma_{A=a} R$ , which is an important component in relationship queries. To avoid decompressing the whole column, we consider the variant of RLE – compressing the repeats of the same element as (value, start-position). Assume the corresponding encoded pairs for values  $a$  and  $a + 1$  are  $(a, s)$  and  $(a + 1, s')$  respectively. Then the answers of  $\pi_B \sigma_{A=a} R$  are the values in column  $B$  from position  $s$  to position  $s' - s$ . OMC adopts this variant of RLE on sorted columns, e.g., **DT . Term** .

**Bitmap encoding.** A bitmap index consists of a set of bit-vectors. Each bitvector indicates the occurrences of one distinct value of the indexed attribute. That is, for each distinct value  $t$ , one bitvector is maintained. The  $i$ -th position of the bitvector is set to ‘1’ if  $t$  appears at the  $i$ -th position in the original column and ‘0’ otherwise. It is efficient to perform bitwise operations – AND, OR, XOR and NOT on bitmap index. To further reduce the size of the bitmaps, literature [33, 58, 9] applies run-length encoding(RLE) on them. Interestingly, The bitwise operations can still be issued directly on the compressed bitmaps without decompressing. Two outstanding techniques are byte-aligned bitmap compression (BBC) [9] and word-aligned hybrid (WAH) compression [58, 56]. However, the bitmap scheme is recommended to apply only on columns with low cardinality, say around 50 [4]. OMC does not use bitmap encoding, since the cardinalities of columns in our datasets are generally high and RLE achieves better performance compared with bitmap.

## 2.1 Compiling Code for SQL Queries

Generating and compiling code has been studied widely in order to improve the performance [8, 41, 39]. For example, DBToaster[8] compiles SQL queries into C++ code for view maintenance problem in order to provide fast delta processing. [41] compiles TPC-H style analytics queries to LLVM bytecode and C. In addition, [39] generates in-memory pipelined hash-join query plans in C++ directly from Datalog queries for path-counting queries. In this paper, we provide a code generator to generate C++ code for relationship queries.

## 2.2 Graph Databases

Relationship queries are a superset of graph reachability queries, so one possible solution is to apply existing graph databases. Graph databases have become ubiquitous with the advancement and popularity of social networking. Some prominent ones include Apache Giraph [1], GPS [48], GraphLab [2], and Neo4j [55] [23]. The

first three adopt vertex-centric programming models, which supports asynchronous computation and prioritized scheduling, but do not offer declarative query interface and can not express simple relational idioms [39]. Neo4j provides its own graph Cypher query language, which can express relationship queries. Therefore, we employ Neo4j as a baseline system in our experiments. [34] provides the Cypher statements for the SQL relationship queries of this paper.

## 2.3 Execution Model

To answer an SQL query, database systems first translate the query into a physical query plan, then evaluate this physical query plan to produce result. The traditional way to evaluate this physical query plan is the iterator model [35, 44, 22]. In the iterator model, every physical algebraic operator conceptually generates a tuple stream from its input, and iterating over this tuple stream by repeatedly calling the *next* function of the operator. This iterator model is a simple interface, which allows for easy combination of arbitrary operators, and is a good choice when query processing is dominated by I/O and CPU consumption is less important. As main memory grows, query performance is more and more determined by the CPU costs. The iterator model shows poor performance on modern CPUs due to lack of locality and frequent instruction mis-predictions[41].

Since CPU costs are a critical issue for modern main-memory database systems, the iterator model is not the optimal solution any more. Some systems tried to reduce the high calling costs of the iterator model by passing blocks of tuples (batch oriented processing) between operators [43, 41]. This greatly reduces the number of function invocations, but causes additional materialization costs. The MonetDB system [36, 27] materializes all intermediate results, which eliminates the need to call an input operator repeatedly. Besides simplifying operator interaction, materialization has other advantages, but it also causes significant costs. The MonetDB/X100 system [61] chooses a middle ground by passing large vectors of data and evaluating queries in a vectorized manner on each chunk. This offers good performance, but still does not reach the speed of hand-written code[41]. In this paper, GQ-Fast produces C++ hand-written like code directly from the physical query plan of relational queries. GQ-Fast iterators each fragment by using simple loop, since the size of each fragment is calculated in the code generating phase by using meta data.

## 3. ARCHITECTURE

Applications use GQ-Fast as an OLAP-oriented database that accompanies their original, transaction-oriented database. Figure 4 is an overview of GQ-Fast’s architecture.

The *GQ-Fast Loader* receives loading commands and, in response, it retrieves data from a relational database (or databases) and creates a GQ-Fast database<sup>7</sup> and relevant metadata, which contains information about fragments and their encodings. The schema of the GQ-Fast database has to follow certain conventions; see Section 4. The data of a GQ-Fast database is stored into in-memory data structures (see Section 5).

Then the *GQ-Fast Query Processor* receives an SQL query and outputs its result. It consists of several subcomponents. The *Algebra Translator* translates an SQL query into a relational algebra expression, which is then transformed into a *Relationship Query*

<sup>7</sup>Currently, GQ-Fast does not allow incremental update of the loaded data. In the two biomedical knowledge analysis applications, in which GQ-Fast is currently used, this is not an important limitation since datasets change relatively rarely. Hence, it is sufficient to reload an entire GQ-Fast database periodically. Future work will lift this restriction.

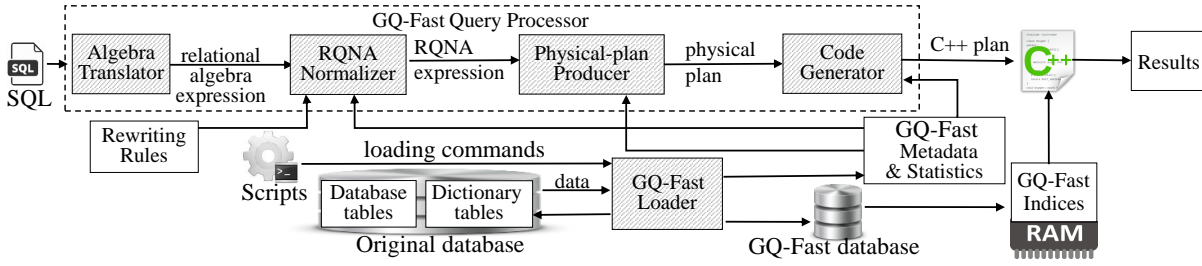


Figure 4: **Architecture of relationship query processing of GQ-Fast**. The *GQ-Fast Loader* produces GQ-Fast database and metadata, the *GQ-Fast Query Processor* receives relationship queries and produces answers.

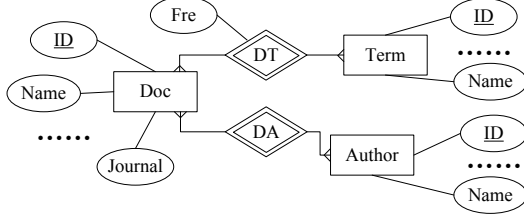


Figure 5: **PubMed ER schema**. **Document** and **Term** (Resp. **Author**) have n-to-n relationship.

*Normalized Algebra (RQNA) expression* (RQNA will be formally defined in Section 4) by the *RQNA Normalizer* by applying rewriting rules. Given an SQL query  $q$  in its algebraic format, the *RQNA Normalizer* applies the following rewriting rules to transform it into RQNA: (1) push every possible selection and projection down to the corresponding tables; projections are upon selections, (2) rewrite into a *left-deep*. The *RQNA Normalizer* is also a verifier who verifies whether an input SQL query is a relationship query by checking the restrictions according to metadata. Afterwards, the valid RQNA expression is transformed into a physical-level plan by the *Physical-plan Producer*. The *Code Generator* consumes the physical plan and metadata and produces a C++ program, which is then compiled and ran on the GQ-Fast index to get final results. GQ-Fast also provides (as JDBC does) the ability to prepare a query statement once and execute it multiple times, changing each time the parameters.

#### 4. RELATIONSHIP QUERIES AND ALGEBRA EXPRESSIONS

FastR supports SQL schemas. It classifies tables into *entity* tables  $E_1, \dots, E_m$  and *relationship* tables  $R_1, \dots, R_n$ . The naming relates to the well-known E/R schema design technique [20]. Intuitively, entity tables correspond to entities of the E/R design, whereas the relationship tables correspond to many-to-many relationships. For example, Figure 5 illustrates the E/R design of the PubMed database. The tables **Doc**, **Term**, **Author** and **Journal** are entity tables. The relationship tables **DT** and **DA** capture the many-to-many relationship between **Doc** and **Term**, and **Doc** and **Author**, respectively.

Entity tables have to follow a single convention: Each FastR entity table must have an integer primary key (aka ID) attribute. In practice, this convention does not limit generality, since database schema designers often follow it. This convention is also recommended when translating an E/R design into a schema [20]. In our examples, the ID attributes are always named **ID**.

$$\begin{aligned}
 RQNA &\Rightarrow \gamma_{k; f_1(\cdot) \mapsto N_1, \dots, f_n(\cdot) \mapsto N_n} Join & (1) \\
 &| & \\
 Join &\Rightarrow Join & (2) \\
 &\Rightarrow Join \bowtie_{j, k_1=v, k_2} (\pi_{\bar{A}}(T \mapsto v)) & (3) \\
 &| & \\
 &| \pi_{\bar{A}}(\sigma_c(T \mapsto v)) & (4) \\
 &| \pi_{\bar{A}}((T \mapsto v) \bowtie_{v, k_1=x, k_2} Context) & (5) \\
 &| & \\
 &| x \text{ is a variable defined by } Context & \\
 Context &\Rightarrow \pi_{v, k} Join & (6) \\
 &| \pi_{v, k} \sigma_{c_1}(T_1 \mapsto v) \cap \dots \cap \pi_{v, k} \sigma_{c_n}(T_n \mapsto v) & (7)
 \end{aligned}$$

Figure 6: **Grammar describing RQNA expressions**.

In the general case, each relationship table  $R(F_1, \dots, F_d, M_1, \dots, M_k)$  has  $d$  foreign key attributes  $F_1, \dots, F_d$ , where each foreign key  $F_i$  refers to the ID of an entity  $E_i$ . The intuition, according to E/R design, is that the foreign key  $F_i$  corresponds to the connection between the many-to-many relationship (that corresponds to the relationship table  $R$ ) and the entity  $E_i$ . To make this connection clear in our examples, the foreign key attribute  $F_i$  has the same name as the entity  $E_i$ . E.g., in the PubMed example, the **Term** foreign key of the **DT** table points to the **ID** of the **Term** table. The relationship table may also have  $k$  attributes  $M_1, \dots, M_k$  that are not foreign keys. They correspond to the attributes of the many-to-many relationship in the E/R design. We call  $M_1, \dots, M_k$  *measure attributes*. For example, the *Fre* attribute of the **DT** table is a measure attribute. As is typical in E/R-based schema design, a one-to-many relationship between entities does not have a corresponding relationship table. Instead, it is captured by including a foreign key attribute to the entity table corresponding to the entity on the “many” side of the relationship. For example, the entity table **Doc** has a *Journal* foreign key attribute, which captures the many-to-one relationship between documents and journals.

**Queries** A relationship query (in its algebraic form) involves  $\sigma$ ,  $\pi$ ,  $\bowtie$ ,  $\bowtie$ ,  $\bowtie$  operators and an optional aggregation at the end. It meets the following restrictions (a) join and semijoin conditions are equalities between (primary or foreign) key attributes and (b) aggregations group-by on a primary key or foreign key. The set of relationship queries includes graph reachability (path finding) queries, where the edges are defined by foreign keys. More generally, it includes tree pattern queries, followed by aggregation.

To efficiently answer relationship queries, GQ-Fast first translates them into RQNA (Relationship Query Normalized Algebra) expressions (see syntax in Figure 6). In the simplest case, an RQNA expression is a left-deep series of joins with a selection and aggregation: In Line 4 the RQNA expression starts with a selection  $\sigma_c(T \mapsto v)$ , that qualifies some entities - we call them the *context*

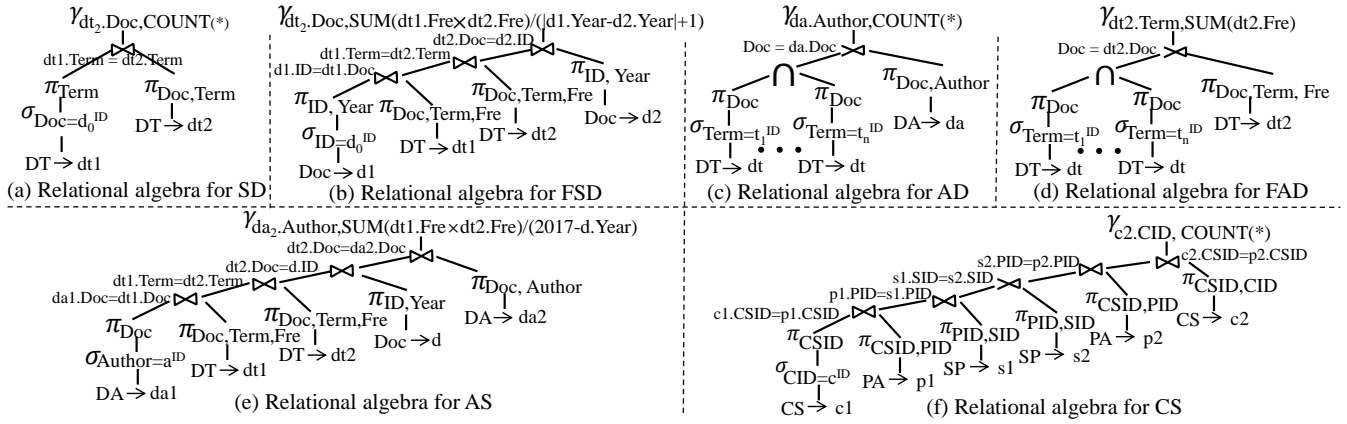


Figure 7: Relational algebra expressions.

entities.<sup>8</sup> Consequently the RQNA expression performs a series of left-deep joins (Line 3) that navigate to entities that relate to the qualifying entities. An RQNA expression may be just the left-deep join (Line 2) or a group-by on the key attribute  $k$  (Line 1), followed by many aggregations. In more complex cases, the SQL query (as shown in examples next) contains “IN (nested query), whereas the IN translates into a semijoin (Line 5). The nested query is itself a relationship query (Lines 6), which is recursively a relationship query or a result of an intersection (Lines 7).

Next we illustrate relationship queries using the datasets of GQ-Fast’s applications: PubMed and SemmedDB. These queries are also used in the experiments and the queries on PubMed dataset are demonstrated in our OLAP dashboard <http://137.110.160.52:8080/demo>.

**EXAMPLE 4.1. [Query SD: Similar Documents]** The Query SD and the corresponding RQNA algebra expression in Figure 7(a) finds documents that are similar to a given document  $d_0$  with ID  $d_0^{ID}$ , where similarity is defined as cosine similarity: Each document  $d$  is associated with a vector  $t^d = [t_1^d, \dots, t_n^d]$ , where  $n$  is the number of terms across all documents. In a frequency-unaware definition,  $t_i^d = 1$  if the document  $d$  contains the  $i$ -th term and  $t_i^d = 0$  otherwise. The cosine similarity between two documents  $x$  and  $y$  is defined as  $\sum_{i=1, \dots, n} t_i^x t_i^y$ .

**Query SD:**  
**SELECT** dt2.Doc, COUNT(\*)  
**FROM** DT dt1 JOIN DT dt2 ON dt1.Term = dt2.Term  
**WHERE** dt1.Doc =  $d_0^{ID}$   
**GROUP BY** dt2.Doc

**[Query FSD: Frequency-and-Time-aware Document Similarity]** The following Query FSD and the corresponding RQNA expression of Figure 7(b) computes time-aware and frequency-aware cosine similarity. In contrast to the frequency-unaware definition of Query SD,  $t_i^d$  is the number of occurrences of the  $i$ th term in document  $d_0$ . Furthermore, the Query FSD raises the similarity degree of documents that are chronologically close.

**Query FSD:**

<sup>8</sup>In a trivial case the condition may be set to true, effectively being absent. We do not discuss this case.

<sup>9</sup>In practice, the queries also normalize for the sizes of  $t^x$  and  $t^y$  and, in later examples, the sizes of measures. The examples exclude the normalizations since they do not present any important additional aspect to the exhibited query pattern.

```

SELECT dt2.Doc,  $\frac{SUM(dt1.Fre * dt2.Fre)}{abs(d1.Year - d2.Year) + 1}$ 
FROM ( ( (Document d1 JOIN DT dt1 ON d1.ID = dt1.Doc)
        JOIN DT dt2 ON dt1.Term = dt2.Term)
        JOIN Document d2 ON d2.ID = dt2.Doc)
WHERE d1.ID =  $d_0^{ID}$ 
GROUP BY dt2.Doc

```

**[Query AS: Author Similarity]** The Query AS and the respective RQNA expression of Figure 7(e) specify an author with ID  $a^{ID}$  and they find other authors that have similar publications, weighing higher those with publications in recent years. The similarity is measured by the frequency-aware cosine of common terms between the publications. It also favors documents that are chronologically close.

**Query AS:**  
**SELECT** da2.Author,  $SUM(dt1.Fre * dt2.Fre) / (2017 - d.Year)$   
**FROM** ( ( (DA da1 JOIN DT dt1 ON da1.Doc=dt1.Doc)
 JOIN DT dt2 ON dt1.Term = dt2.Term)
 JOIN Document d ON dt2.Doc=d.ID)
 JOIN DA da2 ON dt2.Doc=da2.Doc  
**WHERE** da1.Author =  $a^{ID}$   
**GROUP BY** da2.ID

**[Query AD: Authors’ Discovery]** Query AD finds the authors who published papers that pertain to the terms identified by  $t_1^{ID}, \dots, t_n^{ID}$  (e.g., authors that published papers related to “neoplasms” and “statins”). The also displays the number of papers per author. Figure 7(c) shows the RQNA expression.

**Query AD:**  
**SELECT** da.Author, COUNT(\*)  
**FROM** DA da  
**WHERE** da.Doc IN  
 ( **SELECT** dt.Doc **FROM** DT dt **WHERE** dt.Term =  $t_1^{ID}$  )  
**INTERSECT**  
 ⋮  
**INTERSECT**  
 ( **SELECT** dt.Doc **FROM** DT dt **WHERE** dt.Term =  $t_n^{ID}$  )  
**GROUP BY** da.Author

Note that relationship queries do not require that all subqueries have identical structure. Furthermore, the aggregation is not necessary. For example, the following query finds authors who have recently (after 2012) published a paper on “statins” (term id 583352) and at least one of the paper’s authors had also published on “lung neoplasms” (term id 384053).

**SELECT** da.Author

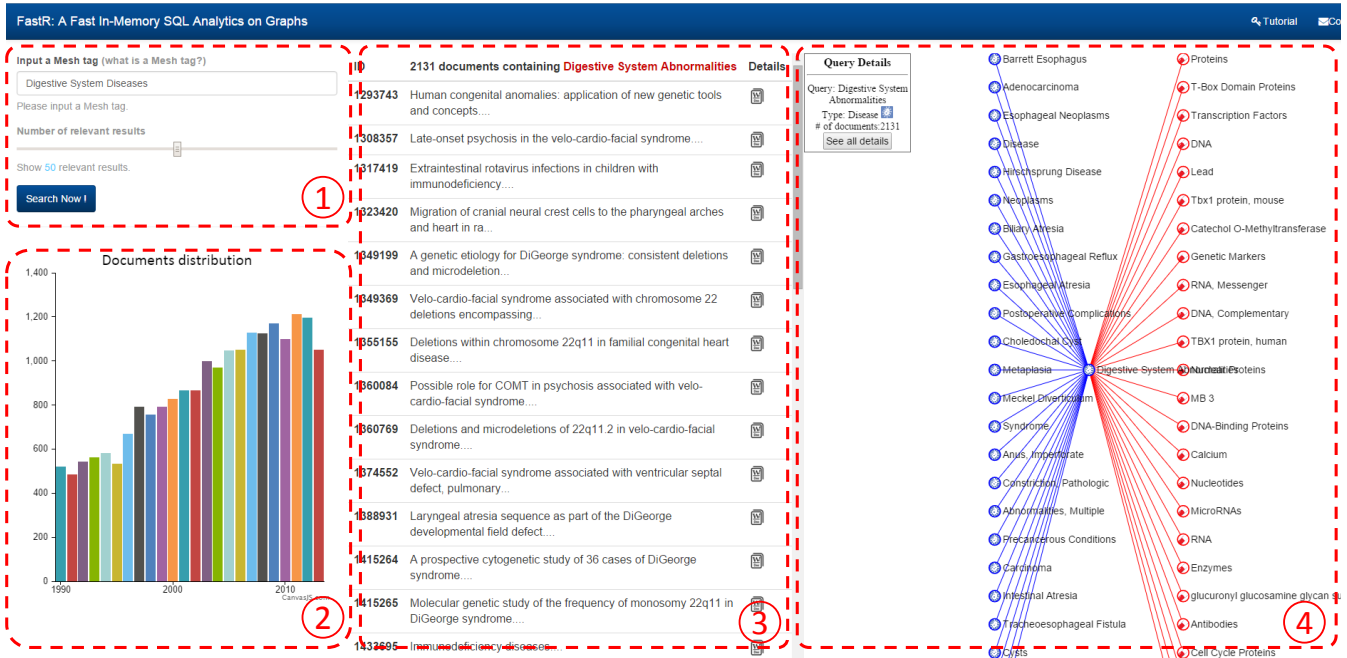


Figure 8: A screenshot of GQ-Fast demo system. ① is the query generator with two components: I. Mesh tag input text box; and II. a slider to limit the number of relevant tags. ② is the exhibitor showing the publication statistics of the query tag. ③ shows a list of documents containing the query tag. ④ is the visual space explorer demonstrating the relevant tags with zoom-in/out, drag and rotation features. Demo link: <http://137.110.160.52:8080/demo>

```

FROM DA da
WHERE da.Doc IN
  ( SELECT dt.Doc FROM DT dt
    WHERE dt.Term = 583352)
INTERSECT
( SELECT d.ID FROM Document d
  WHERE d.Year > 2012)
INTERSECT
( SELECT da.Doc
  FROM DA da JOIN DT dt ON da.Doc = dt.Doc
  WHERE dt.Term = 384053)

```

[Query FAD: Co-Occuring Terms Discovery] Very similarly to the Query AD, the Query FAD finds what (other) terms occur in documents about “neoplasms” and “statins” and how often. Figure 7(d) shows its RQNA expression.

EXAMPLE 4.2. The Scripps Research Institute implemented the Knowledge.Bio<sup>10</sup> [11] system for exploring, learning, and hypothesizing relationships among concepts of the SemMedDB database<sup>11</sup> [30], a repository of semantic predications (subject-predicate-object triples). It currently contains information for approximately 70 million predications from all of PubMed citations. One attractive example in knowledge.bio is that given a patient with, say, a mutation in the Serotonin Reductase (SPR) gene, a collection of Movement Disorders and significantly disrupted sleep, knowledge.bio returns “Serotonin” as a possible treatment by exploring the relevance of those concepts. The biggest challenge of knowledge.bio is the low performance due to the large data size. By applying our GQ-Fast algorithm, the running time of discovering the top-k relevant concepts is dramatically reduced.

<sup>10</sup><http://knowledge.bio/>

<sup>11</sup><http://skr3.nlm.nih.gov/SemMedDB/dbinfo.html>

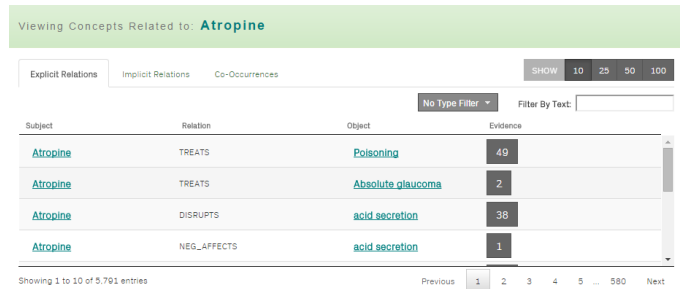


Figure 9: Example application of GQ-Fast in biomedical area.

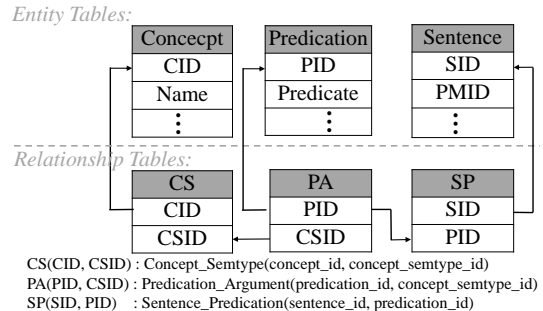


Figure 10: SemmedDB database schema. CS, PA and SP are relationship tables while the others are entity tables.

Figure 9 shows a screenshot of the Knowledge.Bio system. The first result shows that “Atropine” treats “Rattus norvegicus”, according to 319 evidence points. An evidence point is a sentence (in some document) that describes this relation.



Figure 10 shows the schema of SemMedDB. As a use case from Knowledge.Bio, consider the task of finding the concepts that are most relevant to “Atropine”. To answer this query, Knowledge.Bio issues the “concept similarity (CS)” SQL query in, which returns relevant concepts to “Atropine”<sup>12</sup>.

```
CS query:
SELECT c2.CID, COUNT(*)
FROM CS c2, PA p2, SP s2
WHERE s2.PID = p2.PID
      AND p2.CSID = c2.CSID AND s2.SID
IN (
  SELECT s1.SID
  FROM CS c1, PA p1, SP s1
  WHERE s1.PID = p1.PID AND p1.CSID = c1.CSID
      AND c1.CID = c1D)
GROUP BY CID
```

The running time of this query on an Amazon Relational Database Service (Amazon RDS) with MySQL was 25 minutes. GQ-Fast reduced the running time for that query to less than 1 second.

## 4.1 Further Examples

Relationship queries can be found in a variety of applications. Some examples are outlined in the following list.

*Potential Virus Discovery in Network Security* [19, 31]: Consider a database documenting virus infections in a computer network with tables for “virus” entities, “host IP” entities, and virus instance - host IP relationships. To discover potential virus infections for a host who has reported a virus  $s$ , a relationship query first selects the set of hosts associated with  $s$ , and then retrieves and aggregates all the virus infections know for these hosts. The viruses with the high scores might also hide in the host computer.

*Friend Suggestion in Social Networks* [46]: Consider a database with “user” entities, “tweet” entities, and a relationship associating tweets with users. For example, the relationship captures the information that a user read or shared a tweet. To provide friend suggestions for a given user  $u$ , a relationship query first discovers his/her tweets, then returns a sorted list of users based on their association with the discovered tweets.

## 5. GQ-Fast DATA STRUCTURE

Consider a relationship table  $R(D_1, D_2, M_1, \dots, M_m)$ . The GQ-Fast data structure is optimized towards two goals: (i) rapidly evaluating  $\pi_A \sigma_{D_i=c}(R)$ , where  $A$  may be any attribute  $D_j, j \neq i$  or  $M_j$  and (ii) minimizing space by using compressed data structures. The most important mechanism towards compression is *fragments* that encode each  $\pi_A \sigma_{D_i=c}(R)$  using techniques such as compressed bitmaps and Huffman encoding.

For each table of a graph database, GQ-Fast stores two *indices*  $\mathcal{I}_{R.D_1}$  and  $\mathcal{I}_{R.D_2}$ .<sup>13</sup> The only storage pertaining to  $R$  are these indices. The  $\mathcal{I}_{R.D_1}$  index consists of a *lookup data structure* on  $D_1$  and *fragments* corresponding to the other attributes. Given an ID  $c$  and an attribute  $A$ , a *lookup algorithm* uses the data structure to return (i) a pointer to a byte array that encodes the fragment  $\pi_A \sigma_{D_i=c}(R)$  and (ii) the size of the byte array, which is required by the algorithms that decode fragments.

<sup>12</sup>The  $c^{1D}$  is the concept id of “Atropine”

<sup>13</sup>The administrator may elect to store only one of the two indices but then some queries will not be amenable to GQ-Fast’s efficient processing.

**Lookup Data Structure.** Since  $F_1$  is a foreign key, its values are IDs of an entity  $E$ . Therefore, they are integers with a range  $[0, h - 1]$ , where  $h$  is  $|E|$ . Based on this observation, the index  $\mathcal{I}_{R.F_1}$  has one *attribute byte array* for the foreign key attribute  $F_2$  and one *attribute byte array* for each one of the measure attributes  $M_1, \dots, M_m$ . The attribute byte array of an attribute  $A$  stores the fragments  $\pi_A \sigma_{F_1=0}(R), \pi_A \sigma_{F_1=1}(R), \dots, \pi_A \sigma_{F_1=h-1}(R)$  consecutively. Notice that some fragments will be empty.

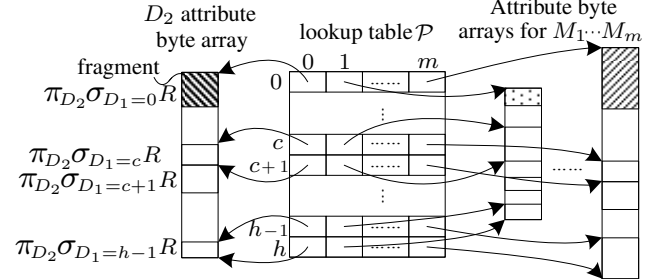


Figure 11: GQ-Fast Index  $\mathcal{I}_{R.F_1}$ . The lookup table stores offsets of fragments. The fragments of different columns have different encodings.

The lookup data structure is a *lookup table*  $\mathcal{P}$ , as illustrated in Figure 11. Each attribute  $F_2, M_1, \dots, M_m$  is associated with a column of the table; e.g.,  $F_2$  is associated with the 0-th column,  $M_1$  with the 1st column, etc. Notice that no column is associated with  $F_1$ . The lookup table has  $h + 1$  rows, with array indices 0 to  $h$ . Cell  $\mathcal{P}[c][a]$  contains a pointer to fragment  $\pi_A \sigma_{F_1=c}(R)$ , where  $a$  is the column number for the attribute  $A$ . The size of the fragment is  $\mathcal{P}[c+1][a] - \mathcal{P}[c][a]$ . There must be a row  $\mathcal{P}[h]$  for computing the size of the last fragment  $\pi_A \sigma_{F_1=h}(R)$ . Notice that by computing the size of fragments from consecutive offsets, GQ-Fast does not need to store fragment sizes explicitly.

For further space savings, the pointers are actually offsets that are represented with the minimum necessary number of bytes. If the fragment byte array of  $A$  has size  $b_A$ , then the offsets pointing to fragments of the byte array, will be integers of size  $\lceil \log_{256} b_A \rceil$  bytes. For example, assume the  $F_2$  attribute byte array (Figure 11) is 3GB and is located at the 64-bit memory address  $0x0000000860A23800$ . Offset values pointing to it will be 4-byte integers, since  $\lceil \log_{256} 3G \rceil = 4$ . Also, assume the offset to the  $c$ -th fragment  $\pi_A \sigma_{F_1=c}(R)$  is  $0x00B09000$  and the offset to the  $c+1$ -st fragment is  $0x00B09100$ . Then, given a request for the fragment  $\pi_A \sigma_{F_1=c}(R)$ , the lookup algorithm returns the start pointer  $\mathcal{F}_{R.A} = 0x0000000860A23800 + 0x00B09000$  and the size  $l = 0x00B09100 - 0x00B09000$ . If this fragment is encoded by an encoding method  $\mathbf{E}$ , GQ-Fast decodes it by using a macro  $\text{decodeE}(\mathcal{F}_{R.A}, l : \mathcal{A}_{R.A}, n)$  to produce a decoded array  $\mathcal{A}_{R.A}$  and the number of elements  $n$  within it. In the following, we introduce encodings for fragments utilized in this paper.

**Retrieve a fragment  $\pi_A \sigma_{F_i=c}(R)$ .** The key feature of GQ-Fast lookup data structure is it can retrieve a fragment efficiently. More precisely, GQ-Fast first obtains an offset-arrays  $\mathcal{P} = \mathcal{I}_{R.F_i}[c]$  by a random access, and its neighbour  $\mathcal{P}_{next} = \mathcal{I}_{R.F_i}[c+1]$ . Then GQ-Fast gets the start address of the fragment  $\mathcal{F}_{R.A} = \mathcal{P}[A]$  and its length  $l = \mathcal{P}_{next}[A] - \mathcal{F}_{R.A}$ . If this fragment is encoded by an encoding method  $\mathbf{E}$ , GQ-Fast decodes it by using a macro  $\text{decodeE}(\mathcal{F}_{R.A}, l : \mathcal{A}_{R.A}, n)$  to produce a decoded array  $\mathcal{A}_{R.A}$  and the number of elements  $n$  within it. In the following, we introduce encodings for fragments utilized in this paper.

**Fragment Encodings.** Fragments are generally encoded by different methods. Unlike column databases, GQ-Fast does not require random access in the compressed data, because GQ-Fast’s query processing either uses all values in a fragment or none of them at all. GQ-Fast currently uses four representative encodings: Uncompressed arrays, bit-aligned compressed array, byte-aligned compressed bitmaps and Huffman-encoded arrays. The latter three have been chosen because (i) each one of them compresses well (and better than the rest) in particular, easy-to-recognize scenarios, and (ii) carefully implemented decoding algorithms have acceptable CPU overhead in the cases of “specialty” of each encoding. Nevertheless, other encodings can also be applied, such as PforDelta [62] that combines aspects of run length encoding and delta encoding.

All fragments of an attribute’s byte array use the same encoding. However, it is allowed (and it is sometimes beneficial) to encode a measure attribute  $M_i$  of a table  $R(D_1, D_2, \dots, M_i, \dots)$  in  $\mathcal{I}_{R.D_1}$  with an encoding method different from the one used in  $\mathcal{I}_{R.D_2}$ . Finally, note that the four encoding methods are used only for numerical values. For string columns, GQ-Fast applies a dictionary encoding that maps strings to integers upon load time, similarly to column databases. In our applications, the dictionary tables that represent the string-to-integer mappings are stored outside main memory, in a conventional database.

GQ-Fast currently uses the following representative encodings:

**Uncompressed Array (UA):** An uncompressed array stores the original numerical values in their declared type, which may be an 8-bit, 16-bit, 32-bit or 64-bit type. Notice that if the index  $\mathcal{I}_{R.D_1}$  encodes an attribute  $A$  as uncompressed array, then the byte array of attribute  $A$  is identical to what the column for  $A$  would be in a column database that stores  $R$  sorted by  $D_1$ .

**Bit-aligned Compressed Array (BCA):** Since GQ-Fast does not require random access within the fragments, the BCA encoding uses fewer than 32 (or 64) bits to store each number of an array. In particular, let us assume that a foreign key attribute  $D$  points to the IDs of an entity  $E$ , which range from 0 to  $h - 1$ . Then each foreign key value needs  $\lceil \log_2 h \rceil$  bits. Consequently, a fragment  $\pi_{A \sigma_{D=c}} R$  with size  $n_c$  takes  $\lceil \frac{n_c \cdot \lceil \log_2 h \rceil}{8} \rceil$  bytes. Notice that the fragment is padded to an integer number of bytes (hence the use of  $\lceil \cdot \rceil$ ) because fragments always take whole bytes, since GQ-Fast needs efficient random access to the start of fragments.

When a measure attribute is dictionary-encoded upon loading, it takes values from 0 to  $m - 1$ , where  $m$  is the number of unique values of  $M$ . Hence, each value is encoded in  $\lceil \log_2 m \rceil$  bits. Finally, if an unsigned integer measure attribute is not dictionary-encoded, its values are encoded in  $\lceil \log_2 r \rceil$ , where  $r$  is the largest value.

**Uncompressed Bitmap (UB):** For each fragment, GQ-Fast maintains a bit array with size  $\mathcal{D} + \Delta'$ , where  $\Delta' \in [0, 7]$  to ensure that fragments are byte-aligned for efficiently accessing a random fragment. Note that the size of an uncompressed bitmap only relies on the domain size and is independent from the fragment size. For example, assume that  $\mathcal{D} = 12$  and a fragment with values  $\{0, 2, 5, 8, 11\}$  should be encoded as 10100100100100000. Note that the size of this bit-array is  $12 + 4 = 16$  rather than 12 since GQ-Fast requires an additional 4 bits. One important and attractive feature of bit-arrays is that intersection operations can be transformed to a logical (bitwise) AND operation.

**Byte-aligned compressed Bitmap (BB):** Bitmaps have been heavily used in analytical processing and provide yet another alternative to uncompressed arrays. Conceptually, given an array  $[v_1, \dots, v_n]$ , where each  $v_i$  is a non-negative integer, the equivalent uncom-

pressed bitmap is a sequence of  $n$  bits, such that the bits at the positions  $v_1, \dots, v_n$  are 1 and all other bits are 0. Bitmap compression methods are based on encoding the length of the (typically long) sequences of zeros that appear between the ones [57, 24]. Compression algorithms differ from each other on the specifics of encoding the lengths. GQ-Fast uses the byte-aligned method to represent a length number [9, 58]. The first bit of a byte is a flag that declares whether (i) the next seven bits are part of a number that also uses consequent bytes or (ii) the remaining seven bits actually represent the length number by themselves. For example, the length numbers for the sequences of zeros in the uncompressed bitmap (UB) are 100, 3000 and 95 respectively.

UB: 000...0001000...0001000...000100  
           100          3000          95  
 BB: 011100100100000111100001001010111010111111

GQ-Fast uses the first byte to represent the length number 100 and the next two bytes for the number 3000 (since  $2^7 < 3000 < 2^{14}$ ). Note that the first bit of the first byte is 1, which means the seven bits in the following byte is still part of the number. Notice that GQ-Fast uses the little endian format, when it represents multi-byte numbers.

**Huffman Encoding:** For attributes with many duplicate values and an uneven frequency distribution, e.g. Zipf distribution, GQ-Fast employs Huffman encoding [53, 52]. GQ-Fast maintains a global Huffman tree, which reflects frequencies in the entire column, but encodes each fragment separately. In addition, GQ-Fast uses an efficient decoding algorithm that avoids tree traversals (i.e., avoids random access on the heap). In lieu of the usual encoding tree, it uses an array as in [17]. This gives performance advantages due to CPU caching (L1 and L2) effects, since an array is a consecutive block of data.

We compare the performance/storage tradeoff of the various encodings analytically and experimentally. The following table summarizes the space needed by each fragment. Assume each fragment contains  $N$  elements and the domain size of the column containing this fragment is  $D$ .

Uncompressed Array (UA)	$32 \cdot N \cdot \lceil \log_{32} D \rceil$
Uncompressed bitmap (UB)	$8 \cdot \lceil \frac{D}{8} \rceil$
Bit-aligned Compressed Array (BCA)	$8 \cdot \lceil \frac{N \cdot \lceil \log_2 D \rceil}{8} \rceil$
Byte-aligned Compressed Bitmap (BB)	$N \cdot (8 \cdot \lceil \log_{128} \frac{D-N}{N} \rceil)$
Huffman	$8 \cdot \lceil \frac{N \cdot E_D + D}{8} \rceil$

where  $E_D = -\sum_{i=1}^D p_i \log p_i$  is the entropy of the column,  $p_i$  is the probability of occurrences of element  $i$ .<sup>14</sup>

Figure 12 shows the most compact way to encode a fragment in key/foreign key columns, as a function of (a) number  $N$  of elements in the fragment (vertical axis), and (b) the size of the underlying domain  $D$  (horizontal axis).<sup>15</sup> Not surprisingly, uncompressed arrays are never the most compact method. (For one, they always take more space than bit-aligned compressed arrays.) In the common cases, where  $D > 2^7$  and  $N \leq D/8$ , compressed bitmaps are more compact than bit-aligned compressed arrays when  $\frac{D}{128^{x+1}} \leq N < \frac{D}{8}$ , for an  $x \geq 1$ .

<sup>14</sup>Here we report the lower bound of the space needed by Huffman. The space needed by Huffman is bounded by  $8 \lceil \frac{N \cdot E_D + D}{8} \rceil$ ,  $8 \lceil \frac{N \cdot E_D + N + D}{8} \rceil$  [40].

<sup>15</sup>Since BCA only applies for fragments containing only unique values.

Figure 12 implies that different fragments of the same column may be most compactly encoded with different methods. For example, a fragment of more documents id’s of a term should be encoded with BB, otherwise, it is less suitable to apply BCA. Though applying different encodings for different fragments can achieve minimal space cost, the penalty is that we need to remember the encoding method for each fragment, which increases the space cost. To balance this trade-off, in this paper, we apply the same encoding (the one with minimal space cost for the fragment with average size) for fragments in the same column. Note that, fragments in different columns still benefit from applying different encodings. And only one encoding type is required to store for each column, which can be stored in the metadata.

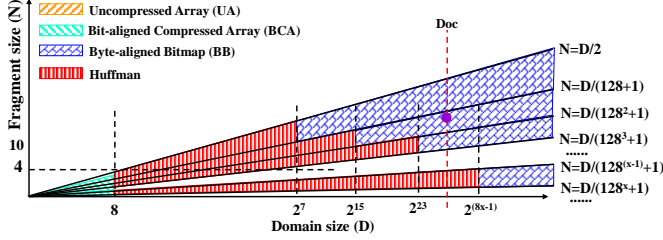


Figure 12: **Space cost comparison of different encodings.** Each area is colored by the compression method with minimal space cost. For example, in the blue area BB compresses the most. The dotted red line with purple circle shows the domain size of **Doc** in the PubMed dataset, which indicates that BB is the best method for **Doc** fragments

## 6. GQ-Fast QUERY PROCESSING

The *GQ-Fast Query Processor* (Figure 4) produces executable C++ source code, as it was illustrated in the introduction. The processor first transforms the given query into an RQNA expression. Then, it translates the RQNA expression into a plan consisting of physical operators. E.g., the plans in Figure 13 correspond to the RQNA expressions in Figure 7. Then the code generator translates the plan into code, using also the metadata provided by the *GQ-Fast Loader*.

Section 6.1 presents the physical operators and the key intuitions in the translation of RQNA expressions into plans. Appendix 9 provides the complete translation algorithm. Then Section 6.2 describes how the GQ-Fast code generator translates plans into code, essentially by mapping each physical operator into an efficient code snippet and stitching these snippets together.

### 6.1 GQ-Fast Physical Operators

GQ-Fast’s physical operators are designed to (i) utilize the GQ-Fast data structure, and (ii) enable code generation to produce bottom-up pipelined execution code. In the following, we explain the physical operators’ syntax and semantics, neglecting for now the bottom-up pipelined execution aspects.

**Fragment-based Join** The operator  $\overset{\rightarrow r.A_1, \dots, r.A_n}{\bowtie}_{B; R \mapsto r} \mathcal{I}_{R, B'} L$  inputs the result of an expression  $L$  that produces a column  $B$ , generally among others. For each value  $b \in B$ , the operator uses the index  $\mathcal{I}_{R, B'}$  to retrieve (and decompress) the fragments  $\pi_{A_i} \sigma_{r.B'=b}(R \mapsto r)$ ,  $i = 1, \dots, n$ . Intuitively  $L$  would be the left operand of a conventional join and  $R \mapsto r$  would be the right side. Conceptually, one may think that the fragments are combined into a result table whose schema has the attributes  $A_1, \dots, A_n$  (and also the attributes of  $L$ ). However, in reality, the decompressed fragments are

not combined into rows. In adherence to the late binding technique [3, 6] of column-oriented processing, the ordering of the items in the fragments dictates how they can be combined into tuples.

The  $\bowtie$  operator is useful for executing both selections and joins of the RQNA expressions:

- A projection/join combination  $\pi_{attrs(L), r.A_1, \dots, r.A_n} (L \bowtie_{B=r.B'} R \mapsto r)$  where  $B$  is an attribute of  $L$  and  $B'$  is a foreign key of a relationship table  $R$  or  $B'$  is the ID of an entity table  $R$ , translates to  $L \overset{\rightarrow r.A_1, \dots, r.A_n}{\bowtie}_{B; R \mapsto r} \mathcal{I}_{R, B'}$ .
- A projection/selection combination  $\pi_{r.A_1, \dots, r.A_n} \sigma_{r.B'=c} (R \mapsto r)$ , where  $c$  is a constant and  $B'$  is a foreign key of a relationship table  $R$  or  $B'$  is the ID of an entity table  $R$ , translates to  $\{[B : c]\} \overset{\rightarrow r.A_1, \dots, r.A_n}{\bowtie}_{B; R \mapsto r} \mathcal{I}_{R, B'}$ . Essentially, GQ-Fast reduces the selection into a join, by considering the left-hand-side argument to be a table with a single tuple and a single attribute  $B$ , whose value is  $c$ .

**Fragment-based Semijoin** The operator  $\overset{\rightarrow r.A_1, \dots, r.A_n}{\bowtie}_{B; R \mapsto r} \mathcal{I}_{R, B'} L$  operates similarly to the fragment-based join but returns only attributes from  $(R \mapsto r)$  if there is a matching tuple in  $L$ . It is introduced in the plan when the RQNA expression has an expression  $\pi_{r.A_1, \dots, r.A_n} ((R \mapsto r) \bowtie_{B=r.B'} L)$ .

The operator maintains a lookup structure for values from the  $B$  column of  $L$ ; for each value  $b \in B$ , the operator checks the lookup structure to find out whether that particular value  $b$  was already received earlier. If it were, then it is dismissed. If this is the first time that  $b$  is received, then the operator marks in the lookup structure that this  $b$  has been received and proceeds to use the index  $\mathcal{I}_{R, B'}$  to retrieve (and decompress) the fragments  $\pi_{r.A_i} \sigma_{r.B'=b}(R \mapsto r)$ ,  $i = 1, \dots, n$ , as the join would. The lookup structure can be a hash set, a tree-based set or an array of booleans whose size is the domain of  $r.B'$ . If  $L$  is relatively large, it is best to use a boolean array, despite the fact that the query needs to initialize all array elements to false. If  $L$  is relatively small, a hash set or a tree is preferable. In the absence of a size estimator, which would estimate the size of  $L$ , GQ-Fast chooses the boolean array approach. The rationale is that the initialization of the array penalizes both fast queries (such as the AD query) and slow queries (such as the CS query) with a few milliseconds (the initialization time in AD and CS are 0.057ms and 121.72ms respectively), which depend exclusively on the size of the underlying domain. Such initialization penalty is unimportant in absolute terms (i.e., the online user experience is not affected by a few milliseconds) but it saves significant lookup cost in the case of the relatively slow queries, where  $L$  is usually large.

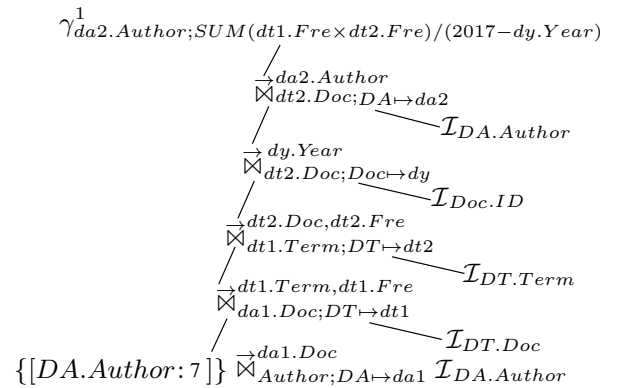


Figure 13: **Example Physical algebraic plan.** This is the physical algebra plan of queries AS.

**Merge Intersection** The operator  $\overset{\theta}{\cap}_{L_1, \dots, L_m}$  computes the result of  $L_1 \cap \dots \cap L_m$ , when each argument  $L_i$  consists of a single sorted attribute. In the case of RQNA queries, an  $L_i$  meets the necessary conditions if it is an expression of the form  $\pi_{l_i, B_i} \sigma_{l_i, K=c}(L_i \mapsto l_i)$ , where  $K$  is a (foreign or primary) key attribute.

The superscript  $\theta = 0$  indicates that the merging should happen directly on the encoded fragments. In a common example, if all the fragments are encoded with compressed bitmap then the merge intersection can be directly applied on the compressed bitmaps. Otherwise,  $\theta = 1$  means fragments  $L_1 \dots L_m$  are encoded with different encodings. Then each fragment needs to be decoded before intersecting by merging. More precisely, a (preallocated, since we know the worst case scenario in advance) array with size  $\min\{|L_1|, \dots, |L_m|\}$  is initialized to store the final intersection results. The operator has pointers pointing to the beginning of each fragment. The pointed-to values are compared: If all the values are the same, then this value is added to the array and all pointers are incremented. Otherwise, all pointers except the one with maximal value are moved forward until the pointed-to values are greater or equal than the maximal one. Then it repeats the above step until all the values in a fragment have been accessed. The operator  $\overset{\theta}{\cap}_{L_1, \dots, L_m}$  is introduced in the plan when the RQNA expression has a series of semijoins and the right arguments of the semijoins are a single sorted column. In particular, an RQNA subexpression  $\pi_{r, A_1, \dots, r, A_n}((R \mapsto r) \times_{r, B'=l_1, B_1} \pi_{l_1, B_1} L_1) \times \dots \times_{r, B'=l_m, B_m} (\pi_{l_m, B_m} L_m)$  translates into the following expression:

$$\overset{\theta}{\times}_{B; R \mapsto r} \overset{\theta}{\cap}_{(\pi_{l_1, B_1} L_1), \dots, (\pi_{l_m, B_m} L_m)} \overset{\theta}{\cap}_{r, A_1, \dots, r, A_n} \mathcal{I}_{R, B'}$$

**Aggregation Operator** The aggregation operator  $\gamma_{r, D; \alpha(s(A_1, \dots, A_n))}^1$  groups its input according to the single group-by attribute  $r.D$  and aggregates the results of the scalar function  $s(A_1, \dots, A_n)$  using the associative aggregation function  $\alpha$  (e.g., **min**, **max**, **count**, **sum**). Recall, in relationship queries the single group-by attribute  $r.D$  is the foreign key of a relationship table or the ID of an entity. In either case, the range of  $r.D$  is the same as the range of the underlying entity ID. Consequently, the  $\gamma^1$  operator's superscript 1 signifies the assumption that the domain of  $G$  is small enough to allow for the allocation of an array, whose size is the domain of  $r.D$  and each entry is a number, initialized to zero. Every time a "tuple" from  $r$  is processed, this array is updated at  $r.D$  accordingly. In addition, an array of booleans registers which values of  $r.D$  were actually found. As was also the case with the lookup structure of the semijoin, it is preferable to incur the penalty of initializing such arrays, instead of using hash sets or tree-based sets that have more expensive lookup times. For example, the aggregation  $\gamma_{Author; \frac{SUM(DT_2.Fre \times DT_1.Fre)}{(2017-DY.Year)}}^1$  of the Query AS, as shown in

Figure 13, initializes an array with size of the domain **Author** to store the aggregated score for each author and also a boolean register array to check which authors are actually accessed.

In non-relationship queries the group-by list may involve more than one group-by attributes, in which case it uses a hash table [20] instead of an array. In other non-relationship queries, the aggregation function  $f$  is non-associative (e.g., the median) in which case it is not enough to allocate an aggregate values' array with just one number per domain entry.

## 6.2 GQ-Fast Code Generator

The GQ-Fast code generator has two main components: to-be-emitted codes boxed by dotted lines in the pseudocode; and control commands that determine which code pieces should be emitted. The inputs of the code generator are (1) physical plan and

### Algorithm 1: FastR Code Generator

```

1 Input: a list of physical operators  $\mathbb{O}$  and metadata  $\mathbb{M}$ ;
2 Output: executable C++ code;
// Initialize arrays in global
3 Initialize an array  $R$  ( $|R| = |r.D$ ) for  $\gamma_{r, D; \alpha(s(A_1, \dots, A_n))}^1$ ;
4 for each semijoin operator  $L \overset{\theta}{\times}_{B; R \mapsto r} \overset{\theta}{\cap}_{r, A_1, \dots, r, A_n} \mathcal{I}_{R, B'}$  do
5   Initialize a boolean array  $\overline{BA}$  ( $|\overline{BA}| = |\overline{R, B'}$ ) with false values;
// Produce codes
6 for each physical operator  $o \in \mathbb{O}$  do
7   if  $o = \{[B : c] \overset{\theta}{\times}_{B; R \mapsto r} \overset{\theta}{\cap}_{r, A_1, \dots, r, A_n} \mathcal{I}_{R, B'}\}$  then
8     offset-array  $\mathcal{P}_r = \mathcal{I}_{R, B'}[c]$ ;
9     for(each column  $r.A_i$ ) {
10       getDecodedFragment( $\mathcal{P}_r, r.A_i, c$ );
11     }
12   else if  $o = L \overset{\theta}{\times}_{B; R \mapsto r} \overset{\theta}{\cap}_{r, A_1, \dots, r, A_n} \mathcal{I}_{R, B'} \mid \mid o = L \overset{\theta}{\times}_{B; R \mapsto r} \overset{\theta}{\cap}_{r, A_1, \dots, r, A_n} \mathcal{I}_{R, B'}$  then
13     //Let  $o'$  be the previous operator of  $o$ 
14     if  $o.B = o'.B$  AND  $o'.R$  is an entity table then
15        $v_B = \mathcal{A}_B[i_B]$ ;
16     else
17       for( $i_B = 0; i_B < n_B; i_B++$ ) {
18          $v_B = \mathcal{A}_B[i_B]$ ;
19       }
20     if  $o = L \overset{\theta}{\times}_{B; R \mapsto r} \overset{\theta}{\cap}_{r, A_1, \dots, r, A_n} \mathcal{I}_{R, B'}$  then
21       if ( $\overline{BA}[v_B] = false$ ) {
22         offset-array  $\mathcal{P}_r = \mathcal{I}_{R, B'}[v_B]$ ;
23         for(each column  $r.A_i$ ) {
24           getDecodedFragment( $\mathcal{P}_r, r.A_i, v_B$ );
25         }
26       }
27   else if  $o = \overset{\theta}{\cap}_{L_1, \dots, L_m}$  then
28     if  $\alpha = 0$  then
29       for(each  $L_i = \{[B : c] \overset{\theta}{\times}_{B; R \mapsto r} \overset{\theta}{\cap}_{r, A_1, \dots, r, A_n} \mathcal{I}_{R, B'}\}$ 
30         offset-array  $\mathcal{P}_r = \mathcal{I}_{R, B'}[c]$ ;
31         fragment  $\mathcal{F}_{r, A} = \mathcal{P}_r[column(A)]$ ;
32       }
33        $I \leftarrow \text{Bitwise}(\mathcal{F}_{r_1, A}, \dots, \mathcal{F}_{r_m, A})$ ;
34     else
35       for(each  $L_i = \{[B : c] \overset{\theta}{\times}_{B; R \mapsto r} \overset{\theta}{\cap}_{r, A_1, \dots, r, A_n} \mathcal{I}_{R, B'}\}$ 
36         offset-array  $\mathcal{P}_r = \mathcal{I}_{R, B'}[c]$ ;
37         getDecodedFragment( $\mathcal{P}_r, r.A, c$ );
38       }
39        $I \leftarrow \text{Merge}(\mathcal{A}_{r_1, A}, \dots, \mathcal{A}_{r_m, A})$ ;
40   else if  $o = \gamma_{r, D; \alpha(s(A_1, \dots, A_n))}^1$  then
41     for( $i_{r, D} = 0; i_{r, D} < n_{r, D}; i_{r, D}++$ ) {
42        $R[i_{r, D}] = \alpha(s(A_1, \dots, A_n))$ ;
43     }
44   Emit corresponding close braces;

Macro getDecodedFragment( $\mathcal{P}_r, r.A, c$ )
1 fragment  $\mathcal{F}_{r, A} = \mathcal{P}_r[column(A)]$ ;
2 offset-array  $next = \mathcal{I}_{R, B'}[c + 1]$ ;
3 length  $l_{r, A} = next[column(A)] - \mathcal{F}_{r, A}$ ;
4 if  $\mathcal{F}_{r, A}$  is UA encoded then
5    $\text{decodeUA}(\mathcal{F}_{r, A}, l_{r, A} : \mathcal{A}_{r, A}, n_{r, A})$ 
6 if  $\mathcal{F}_{r, A}$  is BCA encoded then
7    $\text{decodeBCA}(\mathcal{F}_{r, A}, l_{r, A} : \mathcal{A}_{r, A}, n_{r, A})$ 
8 else if  $\mathcal{F}_{r, A}$  is BB encoded then
9    $\text{decodeBB}(\mathcal{F}_{r, A}, l_{r, A} : \mathcal{A}_{r, A}, n_{r, A})$ 
10 else if  $\mathcal{F}_{r, A}$  is Huffman encoded then
11    $\text{decodeHuffman}(\mathcal{F}_{r, A}, l_{r, A} : \mathcal{A}_{r, A}, n_{r, A})$ 

```

(2) GQ-Fast metadata and statistics, which specifies the encodings of each fragment. The code generator has two phases: (1) initialize necessary buffers (lines 2-5); and (2) emit code pieces for each physical operator (6-44). More precisely, in the first phase,

the GQ-Fast code generator initializes an array  $R$  to store final aggregation results (line 3) and several boolean arrays for duplicate-checking in semijoin operations (lines 4-5). In the second phase, it emits selection codes (lines 8 – 10) for each selection operator  $\{\{B : c\}\} \xrightarrow{r.A_1, \dots, r.A_n} \mathcal{I}_{R.B'}$ . The `getDecodeFragment` macro emits codes for (1) retrieving a fragment (lines 1-3) and (2) calling corresponding decode macros for the fragments (lines 4-11). The encoding information is obtained from metadata. For each join  $L \xrightarrow{r.A_1, \dots, r.A_n} \mathcal{I}_{R.B'}$  and semijoin  $L \xrightarrow{r.A_1, \dots, r.A_n} \mathcal{I}_{R.B'}$  operators (lines 11–26), the generator first checks whether the previous operator operates on an entity table and the operated columns are the same. If yes, then one for-loop can be avoided (lines 13-17). If it is a semijoin operator, then one more duplicate-checking step should be added (line 19). The remaining steps (lines 20-23) of join/semijoin are the same with the selection operator. For each intersection operator  $\cap_{F_1, \dots, F_m}^{\alpha}$ , the generator first identifies whether all the fragments are encoded with the same bitmap encodings by checking the metadata. If yes ( $\alpha = 0$ ), the generator emits codes to perform intersection directly on encoded fragments (lines 27-30). Otherwise, it emits code to perform intersection on decoded fragments (lines 33-36). Then GQ-Fast code generator emit aggregation code pieces (lines 38-40) for the aggregation operator  $\gamma_{r.D; \alpha(s(A_1, \dots, A_n))}^{\alpha}$ . Finally, it emits corresponding close braces in order to produce GQ-Fast algorithm with correct syntax (line 41).

**Memory Requirement.** The required memory size for GQ-Fast is  $4 \cdot |r.D| + \sum_{i=1}^k |r_i.B'|$  bytes, where  $|r.D|$  is the domain size of  $r.D$  for the aggregation operator  $\gamma_{r.D; \alpha(s(A_1, \dots, A_n))}^{\alpha}$ ,  $k$  is the number of semijoin operators, and  $|r_i.B'|$  is the domain size of  $r_i.B'$  for the  $i$ -th semijoin operator  $L \xrightarrow{r.A_1, \dots, r.A_n} \mathcal{I}_{R_i.B'}$ .

**Parallel Computing.** GQ-Fast can use multiple cores/threads to perform parallel computation. The fact that in GQ-Fast (1) each fragment is independent of others, so GQ-Fast can assign fragments to different threads; and (2) the query processing is more CPU-bounded than memory-bounded especially when decompressing encoded fragments. We would like to mention one important technical detail of how to handle two kinds of global arrays, i.e., boolean arrays for each semijoin operation, and a numerical array for aggregation operator. To guarantee the correctness of GQ-Fast, it applies spinlock [13] in each array slot, which is experimentally verified to be more efficient than just using one spinlock on the entire boolean array. For the numerical array, GQ-Fast utilizes the same strategy, which is experimentally verified to be generally faster than maintaining one independent array in each thread than aggregate them together in the main thread (see the experiments in Appendix).

**Discussion.** Relationship queries are mostly CPU-bounded. The bottleneck to answering queries is CPU computation. Some research work [18, 16] indicates that CPU performance is not likely to improve significantly in the future. Thus heterogeneous approaches are introduced to cope with the scalability issue of CPU by using additional computation units. GPU (graphics processor units) is the most representative one due to its commercial availability, full blown programmability and better backward compatibility [59, 25]. We claim that GQ-Fast can be easily applied to GPU environment to further speed up the performance. In particular, each GPU core maintains a complete index. Then elements can be evenly assigned to each core to perform their own computations.

## 7. EXPERIMENTS

We evaluate GQ-Fast’s novelties by running relationship queries

Table name	# rows	Entity ID	Domain Size
<b>DT (Doc, Term, Fre)</b>	207,092,075	<b>Doc</b> (ument)	23,326,299
<b>DT (Doc, Term, Fre)</b>	901,388,401	<b>Term</b>	27,883
<b>DA (Doc, Author)</b>	61,329,130	<b>Term</b>	259,728
<b>Document (ID, Year)</b>	23,176,635	<b>Author</b>	6,301,521

Table	Fragment	Average size	Maximal size	Standard deviation
<b>DT</b>	<b>Doc</b>	7427.18	8192342	197.56
	<b>Term</b>	14.48	667	17.52
<b>DT</b>	<b>Doc</b>	3470.50	8192342	318.72
	<b>Term</b>	63.06	753	39.06
<b>DA</b>	<b>Doc</b>	5.99	5712	21.93
	<b>Author</b>	4.35	3163	8.04
<b>Document</b>	<b>Year</b>	1.00	1	0.00

Table 1: **Data characteristics of PubMed-M and PubMed-MS.** PubMed-MS has larger size of terms than PubMed-M, which results in larger size of **DT** table in PubMed-MS. The gray cells indicates the difference between PubMed-M and PubMed-MS.

Table	# rows	Table	# rows
<b>CS</b>	1550482	<b>Concept</b>	1339227
<b>PA</b>	37508726	<b>Sentence</b>	146055876
<b>SP</b>	81929321	<b>Predication</b>	17359895

Table	Fragment	Ave size	Max size	Standard deviation
<b>CS</b>	<b>concept_semtype_id</b>	1.16	5.00	0.39
	<b>concept_id</b>	1.00	1.00	0.00
<b>PA</b>	<b>predication_id</b>	122.00	109532	845.15
	<b>concept_semtype_id</b>	2.15	38	0.53
<b>SP</b>	<b>sentence_id</b>	4.65	125367	112.36
	<b>predication_id</b>	1.61	140	1.07

Table 2: **Data characteristics of SemmedDB dataset.** SemmedDB has slower fan-out than PubMed.

on three real-life datasets. In all experiments, the full data are located in RAM.

## 7.1 Experimental Setting

The experiments were conducted on a computer with a 4th generation Intel *i7-4770* processor (8M Cache, 8 cores, 3.6 GHz, single socket) running Ubuntu 14.04.1 with 16GB RAM. The size of  $L_1$ ,  $L_2$  and  $L_3$  caches are 256KB, 1MB and 8MB respectively. All the algorithms are coded in C++. The C++ plans were compiled with g++ 4.8.4, using the *-O3* optimization option.

**PubMed Dataset** We use the subset of PubMed publications from 1990 to 2015, which has about 23 million citations for biomedical literature from the National Library of Medicine bibliographic database, life science journals, and online books. The citations in PubMed are labelled by descriptors from MeSH (National Library of Medicine’s controlled vocabulary thesaurus). MeSH contains about 220,000 descriptors (terms), organized in an hierarchy. In addition, PubMed also provides additional descriptors (called *Supplemental*) that also label citations. The number of supplemental terms is around 380,000. Mesh terms are (on average) associated with large number of citations while supplemental terms are (on average) associated with few citations. That is, Mesh term and Supplemental term have different fanout (see formal definition below). Since both space cost and running time are fanout-sensitive, we use two versions of PubMed in our experiments. In one series of experiments, we use PubMed with only Mesh terms, called *PubMed-M*. The second series of experiments, we use PubMed with both Mesh terms and supplemental terms, called *PubMed-MS*.

DEFINITION 7.1. **Fanout.** Given a relationship table  $R$  and a

foreign key  $D$  of it, pointing to the ID of an entity table  $E$ , we define as fanout of  $D$  in  $R$ , also called fanout of  $E.ID$  in  $R$  the ratio of the number of tuples of  $R$ , divided by the number of tuples in  $E$  (which is also the number of unique values of the ID of  $E$ ). The fanout is the expected number of tuples of  $R$  that have a given value of  $E.ID$ .

Table 1 presents the schema and statistics of Pubmed-M and Pubmed-MS: two relationship tables (**DT** (**Doc**, **Term**, **Fre**) and **DA** (**Doc**, **Author**)) and one entity table **Document** (**Doc**, **Year**). The tables **DA** and **Document** are identical in Pubmed-M and Pubmed-MS. The statistics of **DT** differ, depending on whether it is Pubmed-M (white lines) or Pubmed-MS (gray lines). Note that, Pubmed-MS has lower **Term** fanout than Pubmed-M, while Pubmed-MS has larger table sizes than Pubmed-M.

**SemMedDB Dataset.** The Semantic MEDLINE Database (SemMedDB) is a repository of semantic predications (subject-predicate-object triples) extracted by SemRep [45], which is a semantic interpreter of biomedical text. SemMedDB currently contains information about approximately 82.2 million predications from all of PubMed citations (around 25 million citations from 1809 to 2015 June 30th). Table 2 summarizes the data characteristics of SemMedDB dataset.

In the interest of reducing the main memory requirements, the FastR databases for PubMed and SemMedDB do not include strings such as document titles, author names and term names. Rather, they only load data that capture the graph structure of the database and certain measures. (The Postgres and MonetDB databases, which we measure below, also do not store such strings.) In practice, the applications issue SQL queries on FastR to obtain entity IDs and associated measures (see Section 4). Then a conventional database system is used to translate the IDs to printable names. In our experiments, we only consider the FastR part of a query.

**Dataset Summary.** Comparing the fanout and table sizes among these three datasets, we notice that PubMed-M has the highest fanout, while SemMedDB has the lowest fanout. PubMed-MS is the biggest dataset, while SemMedDB is the smallest one.

**Compared Systems.** We compared GQ-Fast with the graph database Neo4j 2.3.2 (enterprise edition), the row-oriented database PostgreSQL 9.4.0 and the column database MonetDB

Neo4j is an open-source NoSQL graph database implemented in Java and Scala. Each entity in entity tables like **Term** is modeled as a vertex, and the attributes of the entity become the attributes of the vertex. Each tuple  $(d_1, d_2, m_1, \dots, m_n)$  in the relationship table, e.g., **DT**, is modeled as an edge between  $d_1$  and  $d_2$ , where  $d_1$  and  $d_2$  are in foreign key columns and  $m_1, \dots, m_n$  are in measure attributes.  $m_1, \dots, m_n$  become the attributes of this edge. Neo4j does not support SQL queries. Section 9.5 shows the translation of the experiments' queries into Cypher<sup>16</sup>, Neo4j's query language.

In the Postgres and MonetDB experiments, entity tables are sorted and indexed on their primary keys. We boost performance by having relationship tables be stored sorted on their first attribute and have indices on all foreign key attributes. We measure the *warm* running time for queries, i.e., each query is run twice and we only report the second measurement. The first one is used just to bring all the necessary data (for the evaluation of the query) into the RAM buffers. Furthermore, we run and average five warm runs.

In addition, PMC and OMC are employed as baselines that isolate the effect of compiled code from the other contributions of GQ-Fast. The PMC maintains one copy of each table, while the OMC maintains two copies of each relationship table sorted by  $F_1$  and  $F_2$  respectively. We manually rewrite the experiments' queries to make optimal use of the sorting. Each column is maintained in an individual array in PMC and OMC. The logical query plans

<sup>16</sup><http://neo4j.com/docs/stable/cypher-query-lang.html>

of PMC/OMC are the same with that of GQ-Fast, i.e., the same RQNA expression. In addition, both PMC and OMC use code generators to produce executable C++ codes.

**Experimental Results** We ran the queries SD, FSD, AD, FAD and AS on PubMed (PubMed-M and PubMed-MS) and the query CS on SemmedDB (see queries in Section 4).

Section 7.2 measures the overall running time performance of each system. Section 7.3 measures the overall space cost for each algorithm/database. The results show that GQ-Fast outperforms MonetDB and OMC by 10-10<sup>3</sup> and 7-70 times respectively, and uses generally less space cost. The benefits of GQ-Fast are gained from the combination of the following effects: (i) the use of compiled code, (ii) bottom-up pipelining execution strategy, (iii) data structure optimized by tuning to the dense IDs, and (iv) applying aggressive data compression schemes. The gap between the speedups of GQ-Fast from MonetDB and that from OMC indicates the power of the use of compiled code. In order to isolate the effect of the other three optimizations in GQ-Fast, we implemented the following variants of GQ-Fast and OMC.

- **GQ-Fast-UA**. It is GQ-Fast with uncompressed array encodings.
- **GQ-Fast-UA(Binary)**. It is GQ-Fast-UA but instead of locating directly to corresponding positions for search values in the lookup structure, GQ-Fast-UA(Binary) uses binary search to find the positions.
- **GQ-Fast-UA(Map)**. It is GQ-Fast-UA but instead of using an array to store the final aggregation results, it uses a hashmap. And it uses a hashmap to replace the boolean array for semi-joins.
- **OMC-denseID**. It is OMC but using arrays instead of hashmaps in both lookup and aggregation. The lookup data structure in OMC-denseID is the same with that in GQ-Fast.

Then we conducted the further experiments in order to isolate the effect of the other three optimizations.

- Measured the effect of GQ-Fast using the dense IDs assumption against GQ-Fast without using it by comparing (i) GQ-Fast-UA vs. GQ-Fast-UA(Binary) in Section 7.4.1, and (ii) GQ-Fast-UA vs. GQ-Fast-UA(Map) in Section 7.4.2.
- Measured the effect of bottom-up pipelining against materializing intermediate results by comparing GQ-Fast-UA vs. OMC-denseID in Section 7.5.
- Analyzed the performance of different compressions in Section 7.6 and evaluated the effect of different number of threads on GQ-Fast performance in Section 7.7.

## 7.2 Overall runtime performance

Table 3 reports the average running time of each query for each system, using 8 threads<sup>17</sup> GQ-Fast outperforms the others for all the queries. We further observed that:

- GQ-Fast outperforms MonetDB and OMC by about 170 times and 20 times on the average (see ratio columns). If GQ-Fast only apply UA compression, it will achieve better performance, e.g., the running time of AS query on PubMed-M is 4.45s.

<sup>17</sup>We applied spinlock [13] to protect the correctness of sharing the arrays for of the semijoin and aggregate operators.

	Query	Join # tuples	Result # tuples	(a)	(b)	(c)	(d)	(e)	(f)	MonetDB	OMC
				Neo4j	Postgres	MonetDB	PMC	OMC	GQ-Fast	GQ-Fast	GQ-Fast
Pubmed-M	SD	22,401,361	6,409,707	14.7	211.2	10.8	23.36	2.47	<b>0.230</b>	47.0	10.7
	FSD	22,401,361	6,409,707	86.6	567.5	23.9	33.98	5.93	<b>0.821</b>	29.1	7.2
	AD	99,734	57,584	7.4	158.1	3.2	4.82	0.73	<b>0.037</b>	86.5	19.7
	FAD	717,487	5,643	18.2	198.6	4.5	7.16	0.88	<b>0.064</b>	70.3	13.8
	AS	147,273,421	6,393,107	5546.5	29520.5	4474.8	5832.30	194.77	<b>5.662</b>	790.3	34.4
Pubmed-MS	SD	136,151,592	12,466,510	61.6	741.2	49.3	400.24	10.25	<b>1.068</b>	46.2	9.6
	FSD	136,151,592	12,466,510	146.8	2148.7	112.8	1892.30	32.80	<b>4.376</b>	25.8	7.5
	AD	85,982	64,765	6.9	112.9	2.7	19.67	0.67	<b>0.035</b>	77.1	19.1
	FAD	1,503,368	9,556	11.1	119.6	3.5	24.99	0.71	<b>0.062</b>	56.5	11.5
	AS	1,391,434,113	9,803,226	9604.8	180164.1	28918.8	33321.74	3083.30	<b>54.720</b>	528.5	56.3
SemmedDB	CS	207,191	5,057	21.0	53.1	4.7	23.58	2.12	<b>0.031</b>	151.6	68.4

Table 3: **End-to-end runtime performance tests (in seconds)**. Numbers in bold are the fastest ones.

	(a)	(b)	(c)	(d)	(e)	(f)	MonetDB	OMC
	Neo4j	Postgres	MonetDB	PMC	OMC	GQ-Fast	GQ-Fast	GQ-Fast
PubMed-M	34.36	20.92	3.69	3.09	3.49	<b>1.47</b>	2.51	2.37
PubMed-MS	112.15	78.90	13.27	11.42	11.82	<b>3.51</b>	3.78	3.37
SemmedDB	10.39	6.84	1.23	<b>0.97</b>	2.05	1.36	0.90	1.51

Table 4: **Space cost for each system (in GB)**. Numbers in bold are the smallest ones.

- MonetDB outperforms Postgres, which is explicable by the analytic nature of relationship queries. MonetDB also outperforms PMC, which means that the performance boost by MonetDB’s indexing is more important than the performance boost by PMC’s compiled code.
- Neo4j beats Postgres in all the queries, which is explicable given the many graph path navigations in relationship queries. Interestingly, MonetDB outperforms Neo4j in almost all cases, which indicates that for such OLAP queries, column-databases are probably favorable to graph databases. The exception is the AS on PubMed-MS, where long relationship paths and relatively low fanout give the edge to Neo4j.
- OMC outperforms MonetDB, since (a) OMC uses code generation and (b) has two copies of each relationship table. For example, OMC uses two copies of the **DT** table in the SD query. Therefore each OMC lookup is a binary search on the sorted column (hence essentially tying the index-based lookups of MonetDB) and the lookups’ results are run-length encoded on the sorted column, hence reducing the size of intermediate results.
- High fanout is favorable to GQ-Fast: The improvement over the competing systems is usually higher in the queries SD, FSD, FAD and AS, when they use the **DT** of Pubmed-M, than it is in the queries that use the **DT** of Pubmed-MS. The difference is the higher fanout of **Term** in the **DT** of PubMed-M. We conjecture that high fanouts amortize over larger fragments the fixed costs of the decompression routines, therefore extending GQ-Fast’s advantages.

### 7.3 Overall space cost

Table 4 presents the overall space costs. GQ-Fast has the lowest space cost in PubMed-M and PubMed-MS. Interestingly, GQ-Fast also uses much less space than PMC even though PMC stores only one copy of each table while GQ-Fast stores two “copies” (i.e., two indices); this indicates the importance of the dense compressions. In SemmedDB, GQ-Fast still uses less space than OMC, but more space than PMC. The reason is the fanout of the SemmedDB (averaging at 1.16), which dilutes the effect of fragment compression since fragments are very small and space is spent on padding them

to full bytes. Though PMC uses marginally smaller space than GQ-Fast in SemmedDB, GQ-Fast is still the best overall choice as it is 760 (i.e., 23.58/0.031) times faster (Table 3).

Both MonetDB and OMC use more space than PMC, since PMC only maintains one copy of data and no indices, while OMC stores two copies of data and MonetDB builds indices. One would expect the space cost of OMC to always be less than twice that of PMC, since OMC utilizes run-length encoding to compress the sorted column of each table. This is the case in PubMed-M and PubMed-MS; indeed OMC has only marginally higher space cost than PMC in the PubMed datasets. However, many tables in SemmedDB have very small fanout. For example, in **CS**, each concept has only 1.16 concept.semtypes associated with it on the average (see Table 2). Therefore, in the case of SemmedDB, the run length encoding, which involves one additional counter/integer, ends up wasting space.

Both Neo4j and Postgres have large space cost, since they build large indices and also spend extra space on maintaining particular data format. For example, Postgres stores additional “header” data for each row. For example, the pure data size for SemmedDB is 0.97 GB, while Postgres spends 4.22GB to store it. Furthermore, the Postgres index size is large. For example, the index size is 9.57 GB in the PubMed-M dataset, while the data is 11.35 GB. Neo4j stores data in nodes and relationships of a multi-graph with pairs of key-value properties.

### 7.4 Effects of the dense IDs

The dense IDs assumption was used to allow GQ-Fast to use arrays for semijoins and aggregations instead of using other data structures like hash index. The two following experiments check its importance.

#### 7.4.1 GQ-Fast-UA vs. GQ-Fast-UA(Binary)

We conducted experiments to evaluate the performance of retrieving fragments in GQ-Fast. Table 5 shows the running time of different queries for GQ-Fast-UA(Binary) and GQ-Fast-UA on PubMed-M and SemMedDB<sup>18</sup>. As shown, GQ-Fast-UA

<sup>18</sup>We achieve similar improvements in PubMed-MS. Due to space limitation, we omit them.

outperforms GQ-Fast-UA(Binary) for all the queries. For example, GQ-Fast-UA saves around 12% running time over GQ-Fast-UA(Binary) for AS query. In addition, we also observed that, queries (FSD, AS and CS) with larger number of lookup requests benefits more compared with queries with smaller number of lookup requests, e.g., SD, AD and FAD.

	Ave # lookups	GQ-Fast-UA(Binary)	GQ-Fast-UA	$\theta$
SD	22	247.94	<b>177.08</b>	28.58%
FSD	21748262	1129.72	<b>435.60</b>	61.44%
AD	23609	38.67	<b>30.33</b>	21.57%
FAD	23609	27.84	<b>25.95</b>	6.79%
AS	58589421	7364.92	<b>4510.11</b>	38.76%
CS	132975	16.21	<b>8.62</b>	46.82%

Table 5: **GQ-Fast-UA vs. GQ-Fast-UA(Binary) (in milliseconds)**. The last column shows the improvements, where  $\theta = \frac{\text{GQ-Fast-UA}}{\text{GQ-Fast-UA(Binary)}}$ .

### 7.4.2 GQ-Fast-UA vs. GQ-Fast-UA(Map)

We measured the benefit of choosing an array for aggregation in GQ-Fast over a hashmap by comparing GQ-Fast-UA with GQ-Fast-UA(Map). As shown in Table 6, GQ-Fast-UA outperforms GQ-Fast-UA(Map) for all the queries. GQ-Fast-UA gains more improvement for the queries with larger output like AS query (GQ-Fast-UA saves about 33% running time) than queries with smaller output like CS query.

	Ave # results	GQ-Fast-UA(Map)	GQ-Fast-UA	$\theta$
SD	27,443,100	908.95	<b>177.08</b>	80.52%
FSD	27,307,529	1342.82	<b>435.60</b>	67.56%
AD	200,679	34.84	<b>30.33</b>	12.94%
FAD	56,518	31.63	<b>25.95</b>	17.96%
AS	20,019,297	7766.83	<b>4510.11</b>	41.93%
CS	5,057	10.06	<b>8.62</b>	14.31%

Table 6: **GQ-Fast-UA vs. GQ-Fast-UA(Map) (in milliseconds)**. The last column shows the improvements where  $\theta = \frac{\text{GQ-Fast-UA}}{\text{GQ-Fast-UA(Map)}}$ .

## 7.5 The effect of pipelining

In this experiment we compared OMC-denseID with GQ-Fast-

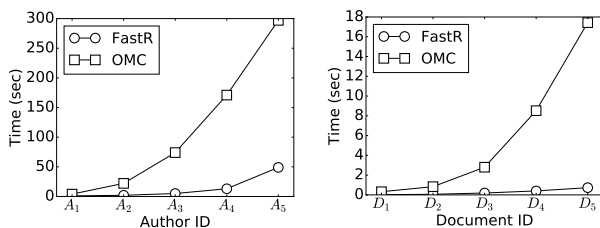


Figure 14: **Avoiding intermediate results**

UA in order to measure the benefit of pipelining over materializing intermediate results. Note that, OMC-denseID and GQ-Fast-UA have the same lookup data structure and same array for final aggregation. Figure 17 reports the running time of GQ-Fast-UA and OMC-denseID on five instances of the AS query, where each instance queries for another author id,  $A_1 - A_5$ . The number of accessed fragments for those queries varies from 7M to 585M (see Table 7). As shown, GQ-Fast-UA outperforms OMC-denseID

by around  $15\times$ . As the number of accessed elements increases, the running time of OMC-denseID increases significantly, since OMC-denseID materializes larger intermediate result columns.

	# of accessed fragments	total # of accessed elements
$A_1$	7,484,532	51,730,682
$A_2$	9,287,804	65,687,183
$A_3$	87,467,470	619,809,092
$A_4$	184,219,134	1,305,764,797
$A_5$	585,932,678	4,153,322,719
$D_1$	78	7,701,798
$D_2$	107	15,002,676
$D_3$	392	61,490,754
$D_4$	476	131,690,364
$D_5$	660	405,002,636

Table 7: **Query statistics**

Figure 17 also shows the performance of GQ-Fast-UA and OMC-denseID for the AD query, with different document ids ( $D_1 \dots D_5$ ) plugged in the **WHERE** clause each time.

## 7.6 Analysis on different encodings

We investigate the performance including compression quality and decompression time of the encoding methods that are employed by GQ-Fast, i.e., uncompressed array (UA), bit-aligned compressed array (BCA), byte-aligned bitmap (BB) and Huffman encoding. Table 8 reports the encoded size of each column in the PubMedMS dataset. As shown, no one encoding is the best for all the columns. Adopting a suitable compression can significantly save space. For example, by using BB, the space cost of **dt1.Term** reduced from 3660.29 MB to 1431.12 MB. The selection of suitable compressions are based on our analysis results in Section 5. For example, as we discussed UA always uses most space. In addition, BB achieves the minimal space on **dt2.Doc**, which indicates the correctness of our analysis.

	UA	BCA	BB	Huffman
<b>dt1.Term</b>	3605.55	2033.25	<b>1376.39</b>	1565.60
<b>dt1.Fre</b>	901.39	454.12	N/A	<b>142.46</b>
<b>dt2.Doc</b>	3605.55	2816.93	<b>1047.71</b>	2779.37
<b>dt2.Fre</b>	901.39	450.74	N/A	<b>134.84</b>
<b>da1.Doc</b>	245.26	198.75	<b>187.54</b>	325.70
<b>da2.Author</b>	245.26	<b>183.95</b>	205.10	275.56
<b>dy.Year</b>	57.17	<b>14.20</b>	N/A	14.29

Table 8: **Size of encoded columns (MB)**. The bold fonts show the minimal space for each column. BB only applies for fragments with unique values, so **dt1.Fre** and **dt2.Fre** can not be encoded by BB.

In addition, we also conducted experiments to evaluate the decompression performance of these encodings for two kinds of fragments: one is fragments on foreign key columns containing only unique values. The other one is fragments on measure attributes, which have many duplicates. For the first case, we generated a **DT** table with **DT.Doc** in zipf distribution with factor  $s = 1.5$  and the domain size is 1 billion. Then we randomly choose 8000 fragments whose sizes are located in [100000-1000, 100000+1000]. We observed from Table 9 that BB achieves the highest compression quality (it saves 69, 25% space) and the highest decompression performance (it is about 30 times faster than Huffman). Huffman has the worst performance, since the domain size is large which requires Huffman to maintain a large decoding table that can not be fitted in L1 or L2 caches.



	# elements per fragment	# fragments	compression ratio	1 thread	2 threads	4 threads	8 threads
BCA	100000 $\pm$ 1000	8000	76.23%	1535.506	864.594	450.890	378.227
BB	100000 $\pm$ 1000	8000	31.75%	1501.806	835.154	428.818	371.442
Huffman	100000 $\pm$ 1000	8000	73.08%	52198.713	29688.662	14934.780	7925.446

Table 9: **Space cost and decompression time of BCA, BB and Huffman.** Domain size is 1 billion, data follows zipf distribution with factor  $s = 1.5$ . Fragments only contain unique values, which simulates fragments in foreign-key columns.

	# elements per fragment	# fragments	compression ratio	1 thread	2 threads	4 threads	8 threads
BCA	10	8000000	21.88%	1647.730	835.046	427.301	363.090
	100	8000000	21.88%	1581.167	801.313	410.039	348.422
	1000	800000	21.88%	1517.293	768.942	393.475	334.347
	10000	80000	21.88%	1456.000	737.880	377.580	320.840
	100000	8000	21.88%	1397.182	708.072	362.327	307.879
	1000000	800	21.88%	1340.741	679.468	347.690	295.442
	10000000	80	21.88%	1286.579	652.020	333.645	283.507
	100000000	8	21.88%	1234.606	625.680	320.167	272.055
Huffman	10	8000000	18.75%	5203.430	2617.872	1318.393	687.644
	100	8000000	15.38%	5055.162	2543.277	1280.826	668.050
	1000	800000	12.34%	4911.119	2470.809	1244.330	649.014
	10000	80000	11.56%	4771.180	2400.405	1208.874	630.521
	100000	8000	11.41%	4635.229	2332.007	1174.428	612.555
	1000000	800	11.39%	4503.152	2265.558	1140.964	595.100
	10000000	80	11.39%	4374.838	2201.003	1108.453	578.143
	100000000	8	11.39%	4250.180	2138.287	1076.868	561.670

Table 10: **Space cost and decompression time of BCA and Huffman.** Domain size is 100, data follows zipf distribution with  $s = 1.5$ . Exist duplicates in each fragment, which simulates fragments in measure columns.

Further, we tested the decompression performance for Huffman and BCA for fragments on measure attributes. We created a **DT** table with **DT.Fre** in zipf distribution with factor  $s = 1.5$  and the domain size is 100. Table 10 reports the decompression time and compression quality for Huffman and BCA with different number of fragments and different size of fragments. As shown, Huffman achieves the highest compression quality and has comparable decompression performance against BCA. Compared with the results in Table 9, we noticed that the decompression performance of Huffman is significantly improved. This is because the domain size is small (say 100) here, which can be fitted into the L1 cache. This result also indicates that Huffman is perfect for measure attributes.

Finally, we observed that multiple threads improve the decompression performance for all the encoding methods. For Huffman, the performance is continuously improved with increasing number of threads, while the improvements of BB and BCA become slower with more threads. This is because Huffman is more CPU bounded than memory bounded.

## 7.7 Effect of multiple threads

At last, we evaluate the effect of multiple threads for the overall performance. Figure 15 shows the running time of AS query on PubMed-M and PubMed-MS and that of CS query on SemmedDB with threads from 1 to 8. We observed that: (1) multiple threads improve the performance; and (2) the improvements are not as significant as expected. This is because there exists skew problem in multiple threads. For example, the difference between the minimal and maximal number of processed fragments in different threads is around 2 million for AS query. The skew problem can be solved by employing load-balance algorithms.

## 8. CONCLUSIONS AND FUTURE WORK

In this paper, we defined and studied relationship queries. GQ-Fast uses a new fragment-based data structure and a new, coordinated bottom-up pipelining execution strategy to answer relationship queries. We itemized the sources of GQ-Fast’s superior per-

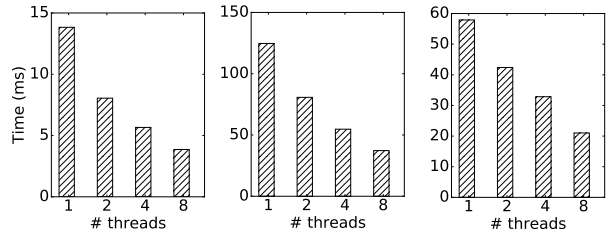


Figure 15: **Running time of AS query on PubMed-M and PubMed-MS, and running time of CS on SemmedDB with threads from 1 to 8.**

formance and measured how much each one of them contributes to the overall performance speedup.

In the future we will study and prototype how GQ-Fast’s data structures and strategy can be incorporated in a general SQL processor, whereas GQ-Fast will be executing relationship subqueries and conventional query processing techniques will be used to further combine and process the results of the relationship subqueries. Furthermore, we will incorporate strategies for skew avoidance and best utilization of the multiple cores.

## 9. APPENDIX

### 9.1 Proof of analytical results

For byte-aligned bitmap, in order to analyze the space cost, we need to know the distribution of elements in the fragment, since the space cost varies with different positions of 1’s in the bitmap. Here we assume the elements are uniformly distributed. Therefore, the expected length of runs is  $\frac{D-N}{N}$ . According to Chernoff Bound [37], the actual length of runs is close to the expected value within  $\epsilon$  with high probability  $1 - e^{-\delta}$ . Therefore, for byte-aligned bitmap, the space cost with high probability is: here, we assume

$N < \frac{D}{2}$  (i.e.,  $\frac{D-N}{N} > 1$ ), which means the number of 1's is less than half of the domain size. If the number of 1's is greater than half of the domain size, then FastR could reverse the bitmap by switching 0 and 1.

In the following, we will compare the space costs of these four encoding methods comprehensively in order to choose the one with minimal space costs. Figure 12 shows the comparison results. The x-axis is the domain size  $D$  and the y-axis is the fragment size  $N$ . The different colors indicate the best encoding methods in terms of space cost for different  $D$  and  $N$ .

Figure 12 is plotted based on the analytical results for these cases:

- Case 1: For any  $D$  and  $N$ ,  $\mathcal{S}_{UA} \geq \mathcal{S}_{BD}$  holds.
- Case 2: If  $D \leq 8$ , then  $\mathcal{S}_{UB} = \min\{\mathcal{S}_{BD}, \mathcal{S}_{BB}, \mathcal{S}_{UA}\}$ .
- Case 3: If  $\frac{D}{128^{x+1}} \leq N < \frac{D}{128^{x-1+1}} (x \geq 2)$  and  $D > 2^{8x-1}$ , then  $\mathcal{S}_{BB} \leq \min\{\mathcal{S}_{UB}, \mathcal{S}_{BD}, \mathcal{S}_{UA}\}$ .
- Case 4: If  $\frac{D}{128^{x+1}} \leq N < \frac{D}{128^{x-1+1}} (x \geq 2)$  and  $D \leq 2^{8x-1}$ , then  $\mathcal{S}_{BD} \leq \min\{\mathcal{S}_{UB}, \mathcal{S}_{BB}, \mathcal{S}_{UA}\}$ .
- Case 5: If  $\frac{D}{128^{x+1}} \leq N \leq \frac{D}{8}$  and  $D > 2^{8x-1}$ , then  $\mathcal{S}_{BB} \leq \min\{\mathcal{S}_{UB}, \mathcal{S}_{BD}, \mathcal{S}_{UA}\}$ .
- Case 6: If  $\frac{D}{128^{x+1}} \leq N \leq \frac{D}{8}$  and  $D \leq 2^{8x-1}$ , then  $\mathcal{S}_{BD} \leq \min\{\mathcal{S}_{UB}, \mathcal{S}_{BB}, \mathcal{S}_{UA}\}$ .
- Case 7: If  $\frac{D}{8} \leq N < \frac{D}{2}$  and  $D > 2^7$ , then  $\mathcal{S}_{UB} = \min\{\mathcal{S}_{BD}, \mathcal{S}_{BB}, \mathcal{S}_{UA}\}$ .

For the rest cases, i.e.,  $\frac{D}{8} \leq N < \frac{D}{2}$  and  $D \leq 2^7$ , Table 11 shows the comparison details.

	Conditions
$\mathcal{S}_{BD} \leq \min\{\mathcal{S}_{UB}, \mathcal{S}_{BB}, \mathcal{S}_{UA}\}$	$N \leq 4$
	$N \leq 5$ AND $32 < D < 64$
	$N \leq 6$ AND $40 < D < 64$
	$N \leq 7$ AND $48 < D < 64$
	$N \leq 8$ AND $48 < D < 64$
	$N \leq 9$ AND $56 < D < 64$
$\mathcal{S}_{UB} \leq \min\{\mathcal{S}_{BD}, \mathcal{S}_{BB}, \mathcal{S}_{UA}\}$	$N \leq 5$ AND $D \leq 32$
	$N \leq 6$ AND $D \leq 40$
	$N \leq 7$ AND $D \leq 48$
	$N \leq 8$ AND $D \leq 48$
	$N \leq 9$ AND $D \leq 56$
	$N \geq 10$

Table 11: Space cost comparisons within  $\frac{D}{8} \leq N < \frac{D}{2}$  and  $D \leq 2^7$ .

FastR maintains a fragment-array (byte-array) to continuously store fragments for each column, which requires the size of each encoded fragment is a multiplication of eight in bits. Therefore, for the UB and BD, we need to add an additional  $\Delta$  ( $\Delta \in [1, 7]$ ) bits to make sure the size meets the requirement of the fragment-array structure. Since FastR applies UB and BD only on fragments with distinct values. Thus, in this section, we focus on discussing the fragment with distinct values, which is the case for foreign key columns. Let  $D$  be the domain size,  $N$  ( $N \leq D$ ) be the number of elements in a fragment. Let  $\mathcal{S}_A$  be the space cost of an encoding method  $A$ .

We provide next the detailed proofs for cases 1 to 7.

PROOF. (Case 1) Recall that  $\mathcal{S}_{UA} = 32 \cdot N \cdot \lceil \log_{2^{32}} D \rceil$  and  $\mathcal{S}_{BD} = N \cdot \lceil \log_2 D \rceil + \Delta$ . Consider  $(2^{32})^i < D \leq (2^{32})^{(i+1)}$  ( $i > 0$ ), then  $\mathcal{S}_{UA} = 32 \cdot (i+1)N$  while  $\mathcal{S}_{BD} \in (32 \cdot iN, 32 \cdot (i+1)N)$ . Therefore for  $\mathcal{S}_{UA} \geq \mathcal{S}_{BD}$ .  $\square$

PROOF. (Case 2) There is at least one element in the fragment, thus  $\mathcal{S}_{BB} \geq 32$ , since UA uses 32 bits for each value. Similarly,  $\mathcal{S}_{BB} \geq 8$  and  $\mathcal{S}_{BD} \geq 8$ , since the size of BB and BD are required to be a multiplication of eight, i.e.,  $\mathcal{S}_{BB} \geq 8$  and  $\mathcal{S}_{BD} \geq 8$ . If  $D \leq 8$  holds, then we have  $\mathcal{S}_{UB} = D \leq 8$ . Therefore,  $\mathcal{S}_{UB} \leq \min\{\mathcal{S}_{UA}, \mathcal{S}_{BB}, \mathcal{S}_{BD}\}$ .  $\square$

PROOF. (Case 3) If  $\frac{D}{128^{x+1}} \leq N < \frac{D}{128^{x-1+1}} (x \geq 2)$  holds, then we have:  $128^{x-1} < \frac{D-N}{N} \leq 128^x$ . Then  $\mathcal{S}_{BB} = 8 \cdot x \cdot N$ . Because  $N < \frac{D}{128^{x-1+1}} < \frac{D}{8 \cdot x}$ , so  $\mathcal{S}_{BB} < D \leq \mathcal{S}_{UB}$ , since  $\mathcal{S}_{UB} = D + \Delta$ . Compare BB with BD.  $\mathcal{S}_{BB} \leq \mathcal{S}_{BD}$  if  $D > 2^{8x-1}$  holds. Because  $\mathcal{S}_{BD} \geq 8 \cdot x \cdot N = \mathcal{S}_{BB}$ . Therefore, If  $\frac{D}{128^{x+1}} \leq N < \frac{D}{128^{x-1+1}} (x \geq 2)$  and  $D > 2^{8x-1}$ , then  $\mathcal{S}_{BB} \leq \min\{\mathcal{S}_{UB}, \mathcal{S}_{BD}, \mathcal{S}_{UA}\}$ .  $\square$

PROOF. (Case 4) If  $D > 2^{8x-1}$  holds, then  $\mathcal{S}_{BD} \leq 8 \cdot x \cdot N = \mathcal{S}_{BB}$ . Recall the proof of Case 3, it is easy to get If  $\frac{D}{128^{x+1}} \leq N < \frac{D}{128^{x-1+1}} (x \geq 2)$  and  $D \leq 2^{8x-1}$ , then  $\mathcal{S}_{BD} \leq \min\{\mathcal{S}_{UB}, \mathcal{S}_{BB}, \mathcal{S}_{UA}\}$ .  $\square$

PROOF. (Case 5)  $\mathcal{S}_{BB} = 8N$  and  $\mathcal{S}_{UB} = D + \Delta$ . Thus  $\mathcal{S}_{BB} \leq \mathcal{S}_{UB}$  since  $D \geq 8N$  holds. If  $D > 2^{8x-1}$ , then  $\mathcal{S}_{BD} > 8N = \mathcal{S}_{BB}$ . Thus If  $\frac{D}{128^{x+1}} \leq N \leq \frac{D}{8}$  and  $D > 2^{8x-1}$ , then  $\mathcal{S}_{BB} \leq \min\{\mathcal{S}_{UB}, \mathcal{S}_{BD}, \mathcal{S}_{UA}\}$ .  $\square$

PROOF. (Case 6)  $\mathcal{S}_{BB} = 8N$  and  $\mathcal{S}_{UB} = D + \Delta$ . Thus  $\mathcal{S}_{BB} \leq \mathcal{S}_{UB}$  since  $D \geq 8N$  holds. If  $D \leq 2^{8x-1}$ , then  $\mathcal{S}_{BD} \leq 8N = \mathcal{S}_{BB}$ , therefore we have: If  $\frac{D}{128^{x+1}} \leq N \leq \frac{D}{8}$  and  $D \leq 2^{8x-1}$ , then  $\mathcal{S}_{BD} \leq \min\{\mathcal{S}_{UB}, \mathcal{S}_{BB}, \mathcal{S}_{UA}\}$ .  $\square$

PROOF. (Case 7) Recall that  $\mathcal{S}_{UB} = D + \Delta$ ,  $\mathcal{S}_{BD} = N \cdot \lceil \log_2 D \rceil + \Delta'$  and  $\mathcal{S}_{BB} = 8N$ . If  $\frac{D}{8} \leq N < \frac{D}{2}$  holds,  $D \leq 8N$ , thus  $D + \Delta \leq 8N$ . The reason is that  $8N$  is a multiplication of eight, so if  $D = 8N$ ,  $\Delta = 0$ . Therefore  $\mathcal{S}_{UB} \leq \mathcal{S}_{BB}$ .

Then we compare  $\mathcal{S}_{UB}$  with  $\mathcal{S}_{BD}$ . If  $D > 2^7$ ,  $\mathcal{S}_{BD} \geq 8N + \Delta' > \mathcal{S}_{BB} > \mathcal{S}_{UB}$ . Therefore, we have If  $\frac{D}{8} \leq N < \frac{D}{2}$  and  $D > 2^7$ , then  $\mathcal{S}_{UB} = \min\{\mathcal{S}_{BD}, \mathcal{S}_{BB}, \mathcal{S}_{UA}\}$ .  $\square$

## 9.2 Translation Algorithm

In this section, we introduce the translation algorithm that translates RQNA expressions into physical plans.

### Algorithm 1: Translation Algorithm

- 1 Mapping each  $\pi_{attrs(L), r.A_1, \dots, r.A_n} (L \bowtie_{B=r.B'} R \mapsto r) \in \mathcal{Q}_R$  to  $\mathcal{Q}_P \leftarrow L \xrightarrow{r.A_1, \dots, r.A_n} \mathcal{I}_{R.B'}$ ;
- 2 Mapping each  $\pi_{r.A_1, \dots, r.A_n} \sigma_{r.B'=c} (R \mapsto r)$  to  $\{[B : c]\} \xrightarrow{r.A_1, \dots, r.A_n} \mathcal{I}_{R.B'}$ ;
- 3 Mapping each  $\pi_{r.A_1, \dots, r.A_n} ((R \mapsto r) \times_{B=r.B'} L)$  to  $\xrightarrow{r.A_1, \dots, r.A_n} \mathcal{I}_{R.B'} L$ ;
- 4 Mapping each  $\pi_{r.A_1, \dots, r.A_n} ((R \mapsto r) \times_{r.B'=l_1.B_1} \pi_{l_1.B_1} L_1) \times \dots \times_{r.B'=l_m.B_m} (\pi_{l_m.B_m} L_m)$  to  $\xrightarrow{r.A_1, \dots, r.A_n} \mathcal{I}_{R.B'} \bigcap (\pi_{l_1.B_1} L_1), \dots, (\pi_{l_m.B_m} L_m)$ ;
- 5 Mapping each  $\gamma_{r.D; \alpha(s(A_1, \dots, A_n))} (L)$  to  $\gamma_{r.D; \alpha(s(A_1, \dots, A_n))}^1$ ;

## 9.3 PMC Algorithm

Here we introduce the detailed algorithms for PMC Let  $L$  be the intermediate result produced by previous operator.

(1) For  $\pi_{A_1, \dots, A_n} \sigma_{B=c} (R)$ , PMC Selection (Algorithm 2 (lines 1 – 8)) performs selection operation by scanning the whole column to get row ids (lines 3 ~ 5) and then executes random accesses to

get values (lines 6 ~ 8). Note that, PMC materializes row ids, i.e., map  $A$ .

(2) For  $(\pi_{A_1, \dots, A_n} L) \bowtie_{L.B_1=R_2.B_2} (\pi_{A_1, \dots, A_m} R_2)$ , PMC Join (Algorithm 3 (lines 2 – 11)) is provided to get join results. It first scans column  $R_2.B_2$  for each value in  $L.B_1$  to get row ids (lines 3 – 6), then uses row ids to find values in corresponding rows in other columns (lines 7 – 11);

(3) For  $(\pi_{A_1, \dots, A_n} L) \times_{L.B_1=R_2.B_2} (\pi_{A_1, \dots, A_m} R_2)$ , PMC applies the same algorithm as  $\bowtie$ . The join algorithm only produces results based on the values in  $L.B_1$ , which insures the correctness of the semijoin.

(4) For  $(\pi_A L) \cap (\pi_A R_2)$ , PMC Intersection (Algorithm 4 (lines 2 – 9)) scans column  $R_2.A$  for each value in  $L.A$ .

(5) For  $\gamma_{A,F} L$ , Algorithm Aggregation (Algorithm 5) is called to compute the aggregated score for each value  $t$  by a function  $F$ .

Note that, PMC does not apply optimizations.

---

#### Algorithm 2: Selection $(\pi_{A_1, \dots, A_n} \sigma_{B=c}(R))$

---

```

1 Initialize a map  $\mathcal{R}$ ;
  /* PMC Selection */
2 Initialize a temporary map  $\mathcal{A}$ ;
3 for  $i = 0; i < |B|; i++$  do
4   if  $B[i] == c$  then
5      $\mathcal{A} \leftarrow i$ ;
6 for each  $i \in \mathcal{A}$  do
7   for  $col = 0; col < n; col++$  do
8      $\mathcal{R} \leftarrow A_{col}[i]$ ;
  /* OMC Selection */
9 Do binary search in column  $B$  to find  $(b, s, e)$  where  $b = c$ ;
10 for  $i = s; i < e; i++$  do
11   for  $col = 0; col < n; col++$  do
12      $\mathcal{R} = A_{col}[i]$ ;
13 Return  $\mathcal{R}$ ;

```

---



---

#### Algorithm 3: Join $(\pi_{A_1, \dots, A_n} L \bowtie_{L.B_1=R_2.B_2} \pi_{A_1, \dots, A_m} R_2)$

---

```

1 Initialize a map  $\mathcal{R}$ ;
  /* PMC Join */
2 Initialize a temporary map  $\mathcal{A}$ ;
3 for  $i = 0; i < |L.B_1|; i++$  do
4   for  $j = 0; j < |R_2.B_2|; j++$  do
5     if  $B_1[i] == B_2[j]$  then
6        $\mathcal{A} \leftarrow j$ ;
7   for each  $j \in \mathcal{A}$  do
8     for  $col_1 = 0; col_1 < m; col_1++$  do
9        $\mathcal{R} = R_2.A_{col_1}[j]$ ;
10    for  $col_2 = m; col_2 < (m+n); col_2++$  do
11       $\mathcal{R} = L.A_{col_2-m}[j]$ ;
  /* OMC Join */
12 for  $i = 0; i < |L.B_1|; i++$  do
13   Do binary search in column  $R_2.B_2$  to find  $(b, s, e)$  where
     $b = L.B_1[i]$ ;
14   for  $j = s; j < e; j++$  do
15     for  $col_1 = 0; col_1 < m; col_1++$  do
16        $\mathcal{R} = R_2.A_{col_1}[j]$ ;
17     for  $col_2 = m; col_2 < (m+n); col_2++$  do
18        $\mathcal{R} = L.A_{col_2-m}[j]$ ;
19 Return  $\mathcal{R}$ ;

```

---

## 9.4 OMC Algorithm

---

#### Algorithm 4: Intersection $((\pi_A L) \cap (\pi_A R_2))$

---

```

1 Initialize a map  $\mathcal{R}$ ;
  /* PMC Intersection */
2 flag = 0;
3 for  $i = 0; i < |L.A|; i++$  do
4   for  $j = 0; j < |R_2.A|; j++$  do
5     if  $R_1.A[i] == R_2.A[j]$  then
6        $\mathcal{R} \leftarrow R_1.A[i]$ ;
  /* OMC Intersection */
7  $i=0; j=0$ ;
8 while  $i < |L.A|$  AND  $j < |R_2.A|$  do
9   if  $L.A[i] < R_2.A[j]$  then
10     $i++$ ;
11  else if  $L.A[i] > R_2.A[j]$  then
12     $j++$ ;
13  else
14     $\mathcal{R} \leftarrow L.A[i]$ ;
15     $i++; j++$ ;
16 Return  $\mathcal{R}$ ;

```

---



---

#### Algorithm 5: Aggregation $(\gamma_{A,F} L)$

---

```

  /* PMC and OMC Aggregation */
1 Initialize a map  $\mathcal{R}$ ;
2 Scan  $L.A$  and get the aggregated score  $F(t)$  for each  $t \in A$  based on
  the function  $F$ ;
3  $\mathcal{R} \leftarrow (t, F(t))$ ;
4 Return  $\mathcal{R}$ ;

```

---

OMC utilizes optimizations – sorting, clustering, maintaining copies, and applying compressions – in column databases [3, 50, 4]. Recall that, OMC does not use hash index, since an individual column in a relationship table is not a primary key. We introduce the optimizations in OMC in details:

**Dictionary Encoding** In our experiments, we applied Dictionary encoding to all the columns. Dictionary encodings reduce the amount of data read from main-memory by replacing attribute values with shorter representations (e.g. integers).

**Clustering and sorting** To speedup the lookup operation, one optimization is to sort the columns. Consequently, all the tuples with the same values are stored contiguously. By clustering, all the same values are grouped together. Thus, once the first element of each cluster is retrieved, all the others can be obtained via sequential accesses. Since the column is sorted, the first element can be found by using a binary search algorithm.

**Run Length Encoding** To further improve the lookup performance, Run-Length Encoding (RLE) is employed by OMC for the sorted columns. RLE compresses runs of the same value to a compact singular representation [3, 4]. The state-of-the-art RLE is to replace a run of the same values with a triple  $(t_i, s_i, l_i)$ , where  $t_i$  is a value,  $s_i$  is the first position/row id of  $t_i$ , and  $l_i$  is the number of occurrences of  $t_i$ . For example, if in  $D_1$  column of  $R$ ,  $d_3$  appears 100,000 times and the tuple/row id of the first one is 3,000,000, then the 100,000 terms are represented as one triple  $(d_3, 3,000,000, 100,000)$ . OMC uses binary search to find corresponding RLE  $(t_i, s_i, l_i)$  for value  $t_i$ .

**Two copies** One limitation of sorting and clustering is that columns within one relation can only be sorted and clustered according to one column, since the other columns should maintain the same or-

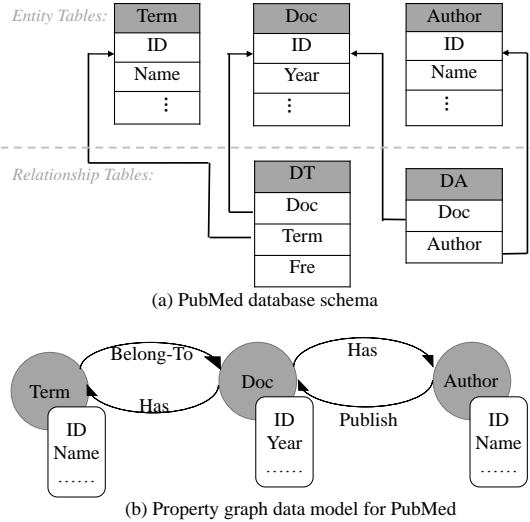


Figure 16: **PubMed database schema and property graph data model for PubMed.** Relationship tables **DT** and **DA** have reference keys pointing to entity tables **Doc**, **Term** and **Author**. For its graph data model, there are three types of vertices **Term**, **Doc** and **Author**, which map to the entities in PubMed. In addition, there are four types of edges **IN**, **HAS**, **INCLUDE**, and **PUBLISH**. Both **IN** and **HAS** edges have one attribute **Fre**.

der to guarantee the correctness of row ids<sup>19</sup>. Therefore, the existing sorting and clustering can only speedup lookup performance for one column. Motivated by the idea of storing different copies to support fault-tolerance in [3, 10], OMC stores two copies for each relationship table  $R$ <sup>20</sup>. In the experiments section, we will show that the two copies optimization will significantly improve performance, though the penalty is more space usage.

**Modifications from PMC to OMC** Though PMC and OMC have the same operator-at-a-time execution model, they have different generated codes for each operator. The main difference between OMC and PMC are summarized as follows:

1. *Binary search vs. whole column scan.* Columns are sorted and clustered, thus OMC can apply binary search instead of full column scan to find row IDs in Algorithm 2 and Algorithm 3. But PMC has to scan whole columns.
2. *Avoiding row ids vs. maintaining row ids.* OMC encodes the sorted columns by RLE, thus each lookup result can be represented as a triple (id, start, end) rather than a list of row IDs in Algorithm 2 and Algorithm 3. Therefore, OMC directly fetch the lookup results by using “start” and “end” positions, while PMC needs to store each row id as they are randomly distributed.
3. *Merge-based intersection vs. nested-loop intersection.* Values in each column are sorted in OMC, thus OMC can call a merge-based intersection instead of using a nested-loop intersection in Algorithm 4. However, PMC has to use nested-loop intersection as the values are not sorted.

## 9.5 Graph database

Figure 16 shows the PubMed database schema and its corresponding graph data model. Note that, each tuple in a relationship

<sup>19</sup>We assume that each column is store separately without maintaining a additional column of row ids. The row ids are omitted and the tuple positions are instead used

<sup>20</sup>Recall that, here we only focus on 2 foreign keys relationship table.

table is translated into an edge. More precisely, a tuple  $(s, t, m_1, \dots, m_n)$  in a relationship table now is an edge between vertices  $s$  and  $t$  with attributes  $m_1, \dots, m_n$  on the edge.

Since Neo4j provides its own declarative graph query language, i.e., Cypher. In order to run our queries on Neo4j, we translate all the queries into Cypher as follows:

## 9.6 Additional Experiments

We conducted experiments to evaluate the performance of different strategies on multi-threading environment, i.e., (1) using spinlock to protect the correctness of sharing the arrays, and (2) maintaining local arrays for each thread, then aggregating them together at last. Currently, GQ-Fast adopts the first design choice. We modified GQ-Fast to use the second choice as GQ-Fast-UA(Non-Share), which is GQ-Fast that only uses uncompressed array encoding and instead of using spinlocks, it maintains local arrays for each thread.

	Ave # results	GQ-Fast-UA(Map)	GQ-Fast-UA	$\theta$
SD	27,443,100	439.63	<b>177.08</b>	73.37%
FSD	27,307,529	671.94	<b>435.60</b>	35.17%
AD	200,679	183.40	<b>30.33</b>	83.46%
FAD	56,518	<b>21.65</b>	25.95	-19.86%
AS	20,019,297	<b>3577.60</b>	4510.11	-26.07%
CS	5,057	25.38	<b>8.62</b>	66.04%

Table 12: **GQ-Fast-UA vs. GQ-Fast-UA(Non-Share) (in milliseconds).** The last column shows the improvements where  $\theta = \frac{\text{GQ-Fast-UA}}{\text{GQ-Fast-UA(Non-Share)}}$ .

As shown in Table 12, none of them always wins the other one. However, GQ-Fast-UA generally achieves higher speedup than GQ-Fast-UA(Non-Share) (see the last column). Therefore, GQ-Fast selects the first design choice.

## 10. REFERENCES

- [1] <http://giraph.apache.org>.
- [2] <http://graphlab.org>.
- [3] D. Abadi, P. A. Boncz, S. Harizopoulos, S. Idreos, and S. Madden. The design and implementation of modern column-oriented database systems. *Foundations and Trends in Databases*, 5(3):197–280, 2013.
- [4] D. Abadi, S. Madden, and M. Ferreira. Integrating compression and execution in column-oriented database systems. In *SIGMOD*, pages 671–682, 2006.
- [5] D. J. Abadi. *Query execution in column-oriented database systems*. PhD thesis, Massachusetts Institute of Technology, 2008.
- [6] D. J. Abadi, P. A. Boncz, and S. Harizopoulos. Column oriented database systems. *PVLDB*, 2(2):1664–1665, 2009.
- [7] D. J. Abadi, S. R. Madden, and N. Hachem. Column-stores vs. row-stores: how different are they really? In *SIGMOD*, pages 967–980, 2008.
- [8] Y. Ahmad and C. Koch. DBToaster: A SQL compiler for high-performance delta processing in main-memory databases. *PVLDB*, 2(2):1566–1569, 2009.
- [9] G. Antoshenkov. Byte-aligned bitmap compression. In *DCC*, page 476, 1995.
- [10] A. Avizienis and J. P. Kelly. Fault tolerance by design diversity: Concepts and experiments. *Computer*, 17(8):67–80, 1984.
- [11] M. N. Bainbridge, W. Wiszniewski, D. R. Murdock, J. Friedman, C. Gonzaga-Jauregui, I. Newsham, J. G. Reid, J. K. Fink, M. B. Morgan, M.-C. Gingras, et al. Whole-genome sequencing for optimized patient management. *Science translational medicine*, 3(87):87re3–87re3, 2011.
- [12] E. Bertino, B. C. Ooi, R. Sacks-Davis, K.-L. Tan, J. Zobel, B. Shidlovsky, and D. Andronico. *Indexing techniques for advanced database systems*. Springer, 2012.

	SQL Queries	Cypher Queries
SD	<pre>SELECT dt2.Doc, COUNT(*) FROM DT dt1 JOIN DT dt2 ON dt1.Term = dt2.Term WHERE dt1.Doc = d<sub>0</sub><sup>ID</sup> GROUP BY dt2.Doc</pre>	<pre>MATCH (n1:Doc{id:d<sub>0</sub><sup>ID</sup>})-[r1:HAS]-&gt;(n2)-[r2:IN]-&gt;(n3) RETURN n3, count(*)</pre>
FSD	<pre>SELECT dt2.Doc, SUM(dt1.Fre + dt2.Fre) abs(d1.Year-d2.Year)+1 FROM ((Document d1 JOIN DT dt1 ON d1.ID = dt1.Doc) JOIN DT dt2 ON dt1.Term = dt2.Term) JOIN Document d2 ON d2.ID = dt2.Doc) WHERE d1.ID = d<sub>0</sub><sup>ID</sup> GROUP BY dt2.Doc</pre>	<pre>MATCH (n1:Doc{id:d<sub>0</sub><sup>ID</sup>})-[r1:HAS]-&gt;(n2)-[r2:IN]-&gt;(n3) RETURN n3, abs(n1.year - n3.year + 1)</pre>
AD	<pre>SELECT da.Author, COUNT(*) FROM DA da WHERE da.Doc IN ( SELECT dt.Doc FROM DT dt WHERE dt.Term = t<sub>1</sub><sup>ID</sup> INTERSECT : INTERSECT ( SELECT dt.Doc FROM DT dt WHERE dt.Term = t<sub>n</sub><sup>ID</sup> GROUP BY da.Author</pre>	<pre>MATCH (t1{id:t<sub>1</sub><sup>ID</sup>})-[r1:IN]-&gt;(d) WITH d : MATCH (tn{id:t<sub>n</sub><sup>ID</sup>})-[rn:IN]-&gt;(d) WITH d MATCH (d)-[r:INCLUDE]-&gt;(a) WITH a, count(a) as count RETURN a, count;</pre>
FAD	<pre>SELECT dt2.Term, SUM(dt2.Fre) FROM DT dt2 WHERE da.Doc IN ( SELECT dt.Doc FROM DT dt WHERE dt.Term = t<sub>1</sub><sup>ID</sup> INTERSECT : INTERSECT ( SELECT dt.Doc FROM DT dt WHERE dt.Term = t<sub>n</sub><sup>ID</sup> GROUP BY da.Author</pre>	<pre>MATCH (t1{id:t<sub>1</sub><sup>ID</sup>})-[r1:IN]-&gt;(d) WITH d : MATCH (tn{id:t<sub>n</sub><sup>ID</sup>})-[rn:IN]-&gt;(d) WITH d MATCH (d)-[r:HAS]-&gt;(t) WITH t, SUM(r.fre) as agg RETURN t, agg</pre>
AS	<pre>SELECT da2.Author, SUM(dt1.Fre*dt2.Fre)/(2017-d.Year) FROM ((DA da1 JOIN DT dt1 ON da1.Doc=dt1.Doc) JOIN DT dt2 ON dt1.Term = dt2.Term) JOIN Document d ON dt2.Doc=d.ID) JOIN DA da2 ON dt2.Doc=da2.Doc WHERE da1.Author = a<sup>ID</sup> GROUP BY da2.ID</pre>	<pre>MATCH (a1 {id:a<sup>ID</sup>})-[r1:PUBLISH]-&gt;(d) -[r2:HAS]-&gt;(t)-[r3:IN]-&gt;(d2)-[r4:INCLUDE]-&gt;(a2) RETURN a2, sum(r2.fre * r3.fre)/(2007 - d.year)</pre>
CS	<pre>CS query: SELECT c2.CID, COUNT(*) FROM CS c2, PA p2, SP s2 WHERE s2.PID = p2.PID AND p2.CSID = c2.CSID AND s2.SID IN ( SELECT s1.SID FROM CS c1, PA p1, Sp s1 WHERE s1.PID = p1.PID AND p1.CSID = c1.CSID AND c1.CID =c<sup>ID</sup>) GROUP BY CID</pre>	<pre>MATCH (c1 {id:c<sup>ID</sup>})-[r1]-&gt;(p1)-[r2]-&gt;(s) WITH s MATCH (s)-[r3]-&gt;(p2)-[r4]-&gt;(c2) RETURN c2, count(*)</pre>

Figure 17: The equivalent Cypher expressions of the relationship queries employed in this paper.

- [13] J. Catozzi and S. Rabinovici. Operating system extensions for the teradata parallel vldb. In *Vldb*, pages 679–682, 2001.
- [14] C. Chen, X. Yan, F. Zhu, J. Han, and S. Y. Philip. Graph OLAP: a multi-dimensional framework for graph data analysis. *KAIS*, 21(1):41–63, 2009.
- [15] C. Chen, X. Yan, F. Zhu, J. Han, and P. S. Yu. Graph OLAP: Towards online analytical processing on graphs. In *ICDM*, pages 103–112, 2008.
- [16] E. S. Chung, P. A. Milder, J. C. Hoe, and K. Mai. Single-chip heterogeneous computing: Does the future include custom logic, fpgas, and gpgpus? In *MICRO*, pages 225–236, 2010.
- [17] K. Chung and J. Wu. Level-compressed huffman decoding. *TCOM*, 47(10):1455–1457, 1999.
- [18] H. Esmailzadeh, E. Blem, R. S. Amant, K. Sankaralingam, and D. Burger. Dark silicon and the end of multicore scaling. In *ISCA*, pages 365–376, 2011.
- [19] E. J. Franczek, J. T. Bretscher, and R. W. Bennett III. Computer virus screening methods and systems, Nov. 16 1999. US Patent 5,987,610.
- [20] H. Garcia-Molina, J. D. Ullman, and J. Widom. *Database Systems: The Complete Book*. Prentice Hall Press, Upper Saddle River, NJ, USA, 2 edition, 2008.
- [21] M. Golfarelli, D. Maio, and S. Rizzi. Conceptual design of data warehouses from E/R schemes. In *HICSS*, volume 7, pages 334–343, 1998.
- [22] G. Graefe. Query evaluation techniques for large databases. *CSUR*, 25(2):73–169, 1993.
- [23] Y. Guo, A. L. Varbanescu, A. Iosup, C. Martella, and T. L. Willke. Benchmarking graph-processing platforms: a vision. In *Proceedings of the 5th ACM/SPEC international conference on Performance engineering*, pages 289–292, 2014.
- [24] G. Guzun, G. Canahuate, D. Chiu, and J. Sawin. A tunable compression framework for bitmap indices. In *ICDE*, pages

- 484–495, 2014.
- [25] B. He and J. X. Yu. High-throughput transaction executions on graphics processors. *PVLDB*, 4(5):314–325, 2011.
- [26] D. A. Huffman et al. A method for the construction of minimum-redundancy codes. *IRE*, 40(9):1098–1101, 1952.
- [27] S. Ideos, F. Groffen, N. Nes, S. Manegold, K. S. Mullender, and M. L. Kersten. MonetDB: Two decades of research in column-oriented database architectures. *DEBU*, 35(1):40–45, 2012.
- [28] B. R. Iyer and D. Wilhite. Data compression support in databases. In *VLDB*, volume 94, pages 695–704, 1994.
- [29] H. Kilicoglu, M. Fiszman, A. Rodriguez, D. Shin, A. Ripple, and T. C. Rindflesch. Semantic medline: a web application for managing the results of pubmed searches. In *SMBM*, volume 2008, pages 69–76, 2008.
- [30] H. Kilicoglu, D. Shin, M. Fiszman, G. Roseblat, and T. C. Rindflesch. SemMedDB: a pubmed-scale repository of biomedical semantic predications. *Bioinformatics*, 28(23):3158–3160, 2012.
- [31] J. Knight. Method and system for remote network security management, Apr. 28 2004. US Patent App. 10/834,443.
- [32] T. J. Lehman and M. J. Carey. A study of index structures for main memory database management systems. In *VLDB*, pages 294–303, 1986.
- [33] D. Lemire, O. Kaser, and K. Aouiche. Sorting improves word-aligned bitmap indexes. *DKE*, 69(1):3–28, 2010.
- [34] C. Lin, B. Mandel, Y. Papakonstantinou, and M. Springer. Fast in-memory SQL analytics on relationships between entities. *CoRR*, abs/1602.00033, 2016.
- [35] R. A. Lorie. *XRM: An extended (N-ary) relational memory*. IBM, 1974.
- [36] S. Manegold, M. L. Kersten, and P. Boncz. Database architecture evolution: mammals flourished long before dinosaurs became extinct. *PVLDB*, 2(2):1648–1653, 2009.
- [37] M. Mitzenmacher and E. Upfal. *Probability and Computing: Randomized Algorithms and Probabilistic Analysis*. Cambridge University Press, 2005.
- [38] B. Momjian. *PostgreSQL: introduction and concepts*, volume 192. Addison-Wesley New York, 2001.
- [39] B. Myers, J. Hyrkas, D. Halperin, and B. Howe. Compiled plans for in-memory path-counting queries. In *IMDM@VLDB*, pages 28–43, 2015.
- [40] G. Navarro and N. Brisaboa. New bounds on D-ary optimal codes. *Information Processing Letters*, 96(5):178–184, 2005.
- [41] T. Neumann. Efficiently compiling efficient query plans for modern hardware. *PVLDB*, 4(9):539–550, 2011.
- [42] D. Nguyen, M. Aref, M. Bravenboer, G. Kollias, H. Q. Ngo, C. Ré, and A. Rudra. Join processing for graph patterns: An old dog with new tricks. In *GRADES*, page 2, 2015.
- [43] S. Padmanabhan, T. Malkemus, A. Jhingran, and R. Agarwal. Block oriented processing of relational database operations in modern computer architectures. In *ICDE*, pages 567–574, 2001.
- [44] F. Porto, O. Tajmouati, V. F. Da Silva, B. Schulze, and F. V. Ayres. Qef-supporting complex query applications. In *CCGRID*, pages 846–851, 2007.
- [45] T. C. Rindflesch and M. Fiszman. The interaction of domain knowledge and linguistic structure in natural language processing: interpreting hypernymic propositions in biomedical text. *JBI*, 36(6):462–477, 2003.
- [46] M. Roth, A. Ben-David, D. Deutscher, G. Flysher, I. Horn, A. Leichtberg, N. Leiser, Y. Matias, and R. Merom. Suggesting friends using the implicit social graph. In *ACM SIGKDD*, pages 233–242, 2010.
- [47] M. A. Roth and S. J. Van Horn. Database compression. *ACM Sigmod Record*, 22(3):31–39, 1993.
- [48] S. Salihoglu and J. Widom. Gps: A graph processing system. In *SSDBM*, page 22. ACM, 2013.
- [49] C. Sapia, M. Blaschka, G. Höfling, and B. Dinter. Extending the E/R model for the multidimensional paradigm. In *ER Workshops*, pages 105–116. Springer, 1999.
- [50] M. Stonebraker, D. J. Abadi, A. Batkin, X. Chen, M. Cherniack, M. Ferreira, E. Lau, A. Lin, S. Madden, E. O’Neil, et al. C-store: a column-oriented DBMS. In *VLDB*, pages 553–564, 2005.
- [51] J. A. Storer. *Data compression: methods and theory*. Computer Science Press, Inc., 1988.
- [52] A. Vinokur. Huffman trees and fibonacci numbers. *Cybernetics and Systems Analysis*, 22(6):692–696, 1986.
- [53] A. Vinokur. Huffman codes and maximizing properties of fibonacci numbers. *Cybernetics and Systems Analysis*, 28(3):329–334, 1992.
- [54] Z. Wang, Q. Fan, H. Wang, K.-L. Tan, D. Agrawal, and A. El Abbadi. Pagrol: parallel graph OLAP over large-scale attributed graphs. In *ICDE*, pages 496–507, 2014.
- [55] J. Webber. A programmatic introduction to neo4j. In *SPLASH*, 2012.
- [56] K. Wu, E. Otoo, and A. Shoshani. On the performance of bitmap indices for high cardinality attributes. In *VLDB*, pages 24–35, 2004.
- [57] K. Wu, E. J. Otoo, and A. Shoshani. Compressing bitmap indexes for faster search operations. In *SSDBM*, pages 99–108, 2002.
- [58] K. Wu, E. J. Otoo, and A. Shoshani. Optimizing bitmap indices with efficient compression. *TODS*, 31(1):1–38, 2006.
- [59] Y. Yuan, R. Lee, and X. Zhang. The yin and yang of processing data warehousing queries on GPU devices. *PVLDB*, 6(10):817–828, 2013.
- [60] P. Zhao, X. Li, D. Xin, and J. Han. Graph cube: on warehousing and OLAP multidimensional networks. In *SIGMOD*, pages 853–864, 2011.
- [61] M. Zukowski, P. A. Boncz, N. Nes, and S. Héman. Monetdb/x100-a dbms in the cpu cache. *IEEE Data Eng. Bull.*, 28(2):17–22, 2005.
- [62] M. Zukowski, S. Heman, N. Nes, and P. Boncz. Super-scalar RAM-CPU cache compression. In *ICDE*, pages 59–59, 2006.